EFFECT OF COMPACTION PRESSURE ON MICROSTRUCTURE AND DENSIFICATION OF ALUMINA-TITANIA COMPOSITE PREPARED BY POWDER METALLURGY ROUTE

by

SITI NURSYUHADA BT YAHAYA

A report submitted in fulfilment of the requirement for the degree of Bachelor of Applied Science (Materials Technology)

FACULTY OF EARTH SCIENCE

UNIVERSITI MALAYSIA KELANTAN

2017

DECLARATION

I declare that this thesis entitled EFFECT OF COMPACTION PRESSURE ON MICROSTRUCTURE AND DENSIFICATION OF ALUMINA-TITANIA COMPOSITE PREPARED BY POWDER METALLURGY ROUTE is the result of my own research except that cited in the references. The thesis has not been accepted for any degree and is not concurrently submitted in candidature of any other degree.

Signature : _____

Name : _____

Date : _____

ACKNOWLEDGEMENTS

First of all, thank you to Universiti Malaysia Kelantan who provides me the laboratory and equipment in order for me to finish my study, that was able me to complete my final year project report.

I would like to take this opportunity to express my deepest gratitude to Dr. Mahani Binti Yusoff as my supervisor for sharing her knowledge in powder metallurgy which is my research topic. She supports me and provides me with useful suggestions, advice and knowledge throughout my thesis completion. She also without hesitate gave me her time to make sure that my thesis is complete. Her continuous support, discussions, comments and advice were the instrumental success of my final year project.

Secondly, I would like to thank Dr. Najmi Binti Masri as my co-supervisor for his guidance and advice throughout the thesis completion and all the lab assistants in Universiti Malaysia Kelantan for guiding me at the beginning phase of this final year project. They are truly dedicate and responsible in helping me.

I also would like to thank my fellow final year project group mates Adillah, Huda, Alya, Farihah and Asma for the beneficial discussion, for their help and support, for the best suggestion and also gave me a fun environment throughout this research. I also want to express my gratitude to my course mate, who supports me and gave me beneficial ideas that were very helpful.

Finally, to my caring, loving and supportive parents and family for gave me their endless support in spiritually throughout my life. Their encouragement and their time are much appreciated. Thank you so much.

EFFECT OFCOMPACTION PRESSURE ON MICROSTRUCTURE AND DENSIFICATION OF ALUMINA-TITANIA NANOCOMPOSITE PREPARED BY POWDER METALLURGY ROUTE

ABSTRACT

In this study, the effect of milling time and compaction pressure on the densification and morphology of Al_2O_3-TiO_2 composite was evaluated. The composite was produces using powder metallurgy route via low energy ball milling and cold compaction. The milling time and compaction pressure was varied at 15, 30, 45 and 60 h and 200, 400, 600 and 800MPa, respectively. The result showed as milling time increased, will produce homogeneous morphology, decrease crystallite size and increased internal strain of Al_2O_3-TiO_2 composite powder. No new phase was formed even at longer milling time (60 h). The densification of Al_2O_3- TiO_2 composite also enhanced with increasing compaction pressure. It was found that the optimum milling time and compaction pressure was during 60 h and at 800 MPa, respectively.

KESAN TEKANAN PEMADATAN TERHADAP MIKROSTRUKTUR DAN KETUMPATAN KOMPOSIT NANO ALUMINA-TITANIA TERHADAP KOMPOSIT DISEDIAKAN MELALUI KAEDAH METALURGI SERBUK

ABSTRAK

Dalam kajian ini, kesan masa kisaran dan tekanan pemadatan terhadap penumpatan dan morfologi Al_2O_3-TiO_2 komposit nano telah dinilai. Komposit yang telah dihasilkan menggunakan kaedah metalurgi serbuk menggunakan bola kisaran tenaga rendah dan pemadatan sejuk. Masa kisaran dan tekanan pemadatan telah divariasikan dengan 15, 30, 45 dan 60 jam dan juga dengan tekanan 200, 400, 600 dan 800MPa. Keputusan menunjukkan peningkatan masa kisaran telah menghasilkan morfologi homogen, pengurangan saiz hablur dan peningkatan terikan dalaman Al_2O_3-TiO_2 serbuk komposit. Tiada fasa baru telah terbentuk walaupun pada masa kisaran lebih lama (60 jam). Penumpatan Al_2O_3-TiO_2 komposit nano juga telah meningkat dengan meningkatnya tekanan pemadatan. Ia didapati bahawa masa kisaran dan tekanan pemadatan optimum ialah pada 60 jam dan pada 800 MPa.

TABLE OF CONTENT

LIST OF FIGURES

LIST OF ABBREVIATIONS

CMC	Ceramic matrix composite
Al_2O_3	Alumina
HIP	Hot isotactic pressing
TiO_2	Titania
MMC	Metal matrix composites
PMC	Polymer matrix composites
C/C	Carbon fibres with carbon matrix
C/SiC	Carbon fibres with silicon carbide matrix
SiC/SiC	Silicon carbide fibres with silicon carbide matrix
THA	Total hip artgroplasty
CVI	Chemical vapour infiltration
P/M	Powder metallurgy
GD	Green density
DP	Densification parameter
XRD	X-ray diffraction
OM	Optical microscopy
m	Mass
V	Volume
AD	Apparent density
TD	Theoretical density
WH	Williamson-Hall
FTIR	Fourier transform infrared

LIST OF SYMBOLS

h	Hours
g	Gram
cm	Centimetre
MPa	Mega Pascal
cps	Count per second
wt%	Weight percent
nm	Nanometre
mm	Millimetre
µm	Micrometre
GPa	Giga Pascal
^oC	Temperature
^{o}	Degree
rpm	Rotation per minute
λ	Lambda
%	Percentage
B_r	overall broadening
Å	ÄngstrÖm
B_i	Instrumental broadening
B_o	Sum of the total broadening of size, lattice strain and instrument
k	Constant
B_{strain}	Broadening due to strain
B_{cryst}	Broadening due to crystallite size
m	Mass
V	Volume

CHAPTER 1

INTRODUCTION

1.1 Background of study

Ceramic materials are inherently resilient to oxidation and deterioration at elevated temperature. It has low fracture toughness. This weakness has been improved significantly by the development of ceramic matrix composites (CMCs) (Callister, 2011).

Alumina (Al_2O_3) has high compressive strength, good chemical and thermal stability (Rocha-rangel *et al.*, 2014). Al_2O_3 also possesses good corrosion and wear resistant. However, due to their brittleness and poor fracture toughness its application as structural material is limited (Oungkulsolmongkol, 2010). Therefore, the addition of secondary ceramic reinforcement phase is one of the techniques to toughen Al_2O_3 (Huang & Nayak, 2014).

CMCs are the combination of reinforcing ceramic with other to achieve a superior properties such as stronger and tougher structure, high strength, and temperature stability (Aigbodion *et al.*, 2010; Low, 2014). Full density and fine microstructure are the basic requirements for high performance of CMCs. Current methods of manufacturing dense particulate reinforced CMCs are liquid phase sintering, hot pressing or hot isotactic pressing (HIP) and liquid-phase sintering (Gutmanas & Gotman, 1999; Callister, 2011).

CMCs are widely used in many industries such as aerospace and electrical industries cutting tools, dental prostheses, thermal barrier coatings, as well as structural materials for the nuclear energy, military, aerospace and building

industries (Aigbodion *et al.*, 2010; Ding, 2014; Low, 2014) due to their excellent properties.

Al_2O_3-based composite is the incorporation of several reinforcement materials such as ceramics, metals and intermetallic into Al_2O_3 matrix forming a composite material (Rocha Rangel, 2010). The reinforcement in Al_2O_3-based composites can be in a form of particulates, whiskers, and short and long fibres (Oungkulsolmongkol, 2010). Al_2O_3-based composite, metal as well as ceramic second phase particles were found to impart an increase in mechanical and thermal shock resistance (Mujahid, 1999; Oungkulsolmongkol, 2010).

Titania (TiO_2) is widely used reinforcement for composites. TiO_2 consist of three common crystal structure called anatase, rutile and brookite (Tan *et al.*, 2012). It is commonly known that rutile is the most stable TiO_2 crystal phase and also the one that is industrially used in many applications. Anatase is metastable at room temperature and shows the highest photocatalytic activity. It also known that anatase TiO_2 displays a higher optical absorption threshold than rutile (Furlani *et al.*, 2014). TiO_2 possesses excellent mechanical resistance, biocompatibility, chemical stability in aqueous environment and chemical inertness. These properties makes TiO_2 is very promising materials for several of medical application especially in orthopaedic and dental implant (Sakka *et al.*, 2014; Tahara *et al.*, 2014). TiO_2 is one of the most efficient semiconducting materials which can be used in applications involving solar energy conversion and storage (Furlani *et al.*, 2014). TiO_2 also can be used in Al_2O_3-based composite. Nanoscale TiO_2 often used in Al_2O_3-based composite because the nano-sized particles can distributed homogeneously within the matrix (Merchant, 2011) and then produce excellent properties.

Some Al_2O_3- based composite has been prepared by different techniques such as self-propagation high temperature synthesis, reaction synthesized, pressure-assisted thermal explosion, slip casting, metal infiltration, sintering high pressing, chemical deposition and powder techniques (Rocha-rangel *et al.*, 2014). Powder processing is recognized as a competitive technology and an alternative to casting or conventional metal forming. The important steps in powder processing are powder mixing, powder compaction and powder sintering. In powder metallurgy, its offers integrity of microstructure, compositional of homogeneity and mechanical property levels equal or better than those of the cast and wrought counterpart (Kuhn, 2012).

1.2 Problem Statement

Al_2O_3-based composite has low toughness and low resistance to mechanical and thermal shocks. Tougher and more reliable Al_2O_3-based composite material can be done by dispersion of ceramic nanoparticles in the composite. TiO_2 offers good compatibility with Al_2O_3 with added advantages to composite such as chemical stability and environmental friendly. Al_2O_3-TiO_2 are both ceramic oxides and Al-Ti system is immiscible, thus prone to have a particle coarsening during sintering. Therefore, a study on compressibility of Al_2O_3-TiO_2 should be carried out because it will affect the densification and flowability in composite.

1.3 Objective

The objectives of this research are:

1. To study the effect of milling time and compaction pressure on the densification and morphology of Al_2O_3-TiO_2 composite produced by low energy ball milling.

2. To investigate the optimum compaction pressure of Al_2O_3-TiO_2 composite prepared by powder metallurgy.

1.4 Expected Outcome

This study will yield the uses of Al_2O_3-TiO_2 composite especially in printing and coating applications which concerns consumer safety and environmental sustainability. The effect of compaction pressure will affect Al_2O_3-TiO_2 composite microstructure and structural properties. Plastic deformation will also occur with the increase in pressure and particles distribution becomes more uniform and finer. The shape of particles will change and the morphology of powder becomes more homogeneous. Also, the composites will increase its density due to low porosity that cause by the compaction.

CHAPTER 2

LITERATURE REVIEW

2.1 Ceramic Materials

Ceramic is composed at least two elements and often more, and their crystal structure are more complex than those for metals. Most ceramics are compound between metallic and non-metallic elements. Ceramics are frequently oxides, nitrides, and carbides. Common ceramic materials include aluminium oxides, silicon dioxides, silicon carbides, silicon nitrides, and also “traditional ceramics”. Those traditional ceramics are of clay, porcelain, as well as cement or glass.

Ceramic materials are relatively stiff and strong, and they are hard. However, ceramic is well-known for their high brittle fracture properties. Brittle fracture consists of the formation and propagation of cracks through the cross section of material in a direction perpendicular to the applied load. Ceramics are widely used in applications that needed high heat resistance for example cookware and cutlery (Callister, 2011). Ceramics are also known for their brittleness properties. Figure 2.1 shows the crack origins and configurations that result from impact (point contact loading), bending, torsional loading and internal pressure (Callister, 2011).

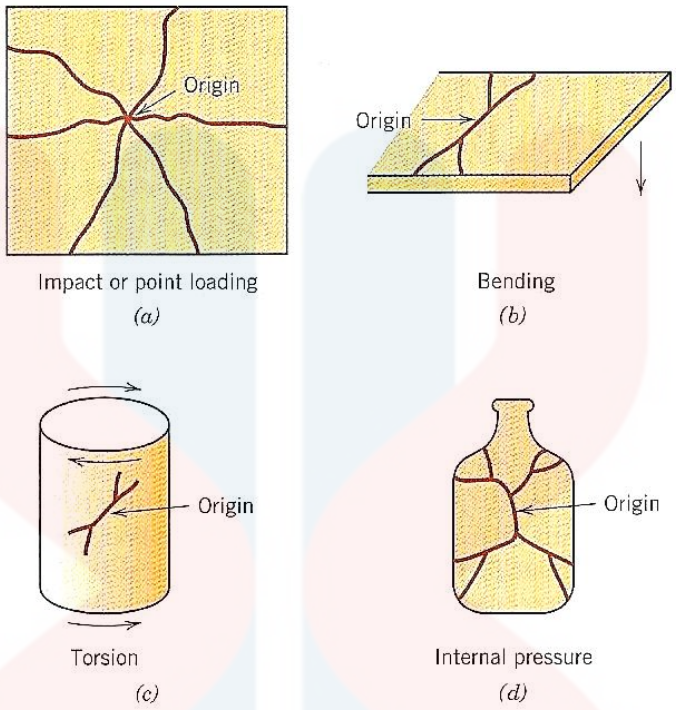

Figure 2.1 : Cracks and configurations of ceramic material (Callister, 2011).

2.2 Strengthening of ceramic materials

Composites may be strengthened by the uniform dispersion of fine particles of a very hard and inert material. The dispersed phase may be metallic or non-metallic, which oxide materials are often used. The strengthening mechanisms involve interaction between the particles and dislocations within the matrix. The dispersed particles are chosen to be unreactive with the matrix phase (Figure 2.2). Impurities atoms that go into solid solution will impose lattice strain on the surrounding host atoms. This will cause the restricted in dislocation movement thus the mechanical strength will be enhanced (Callister, 2011).

The improvement in the fracture properties results from interaction between advancing cracks and dispersed phase particles. Crack initiation normally occurs with the matrix phase, whereas crack propagation is impeded or hindered by the particles, fibres or whiskers (Callister, 2011).

(a) (b)

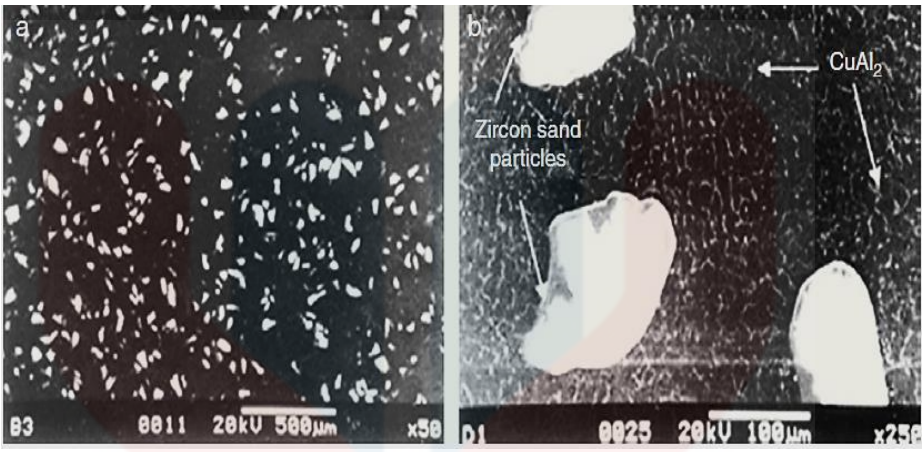

Figure 2.2 : SEM images of composite showing (a) uniform distribution of particles and (b) presence of intermetallic phase (Kumar *et al.*, 2015)

2.3 Ceramic Matrix Composite

Composite is made by combining two or more materials to improve properties. Properties of composites are dependent on the properties of their constituent materials, their distribution and the interaction among them (Banga *et al.*, 2015). Properties of composites which are high strength to weight ratio, resistance to environmental hazards, lower density, high fatigue resistance, and wear resistance has widen the range of application from conventional engineering materials for aerospace to consumer goods (Vijayaraghavan, 2007).

Composite materials can be classified into three categories which are metal matrix composites (MMCs), polymer matrix composites (PMCs) and ceramic matrix composites (CMCs) (Banga *et al.*, 2015). CMCs are the combination of reinforcing ceramic with other to achieve a superior properties such as stronger and tougher structure, high strength, toughness and temperature stability (Aigbodion *et al.*, 2010; Low, 2014). CMC is mostly used in high temperature application such as turbine and jet engines (Aigbodion *et al.*, 2010).

CMCs are usually classified into two materials systems which are oxide-based and non-oxide-based. Oxide-based CMCs consist of an oxide fiber and an oxide matrix such as Al_2O_3/ Al_2O_3 whereas non-oxides can consist of carbon fibers with a carbon matrix (C/C), carbon fibers with a silicon carbide matrix (C/SiC), as well as silicon carbide fibers with a silicon carbide matrix (SiC/SiC) (Sun *et al.*, 1989). The matrices that commonly used are alumina (Al_2O_3), silicon carbide, magnesium oxide, silicon nitride and zirconium oxide.

2.4 Alumina-based composite

A well-known ceramic that are widely investigated is alumina (Al_2O_3). Al_2O_3 is an oxide of aluminium a group III element and very stable and robust material (Vikas, 2006). Al_2O_3 is one of the ceramic that is widely investigate due to its fundamental interest as one of the simplest covalent oxides (Nmr *et al.*, 2013). Al_2O_3 has several allotropic forms, it has internal crystal structure where the oxygen ions are packed in a close-packed hexagonal arrangement (Figure 2.3). Al_2O_3 has a melting temperature of about 2040 °C (Auerkari, 1996).

Al_2O_3 have been used as an ideal bearing surface for prosthetic implants especially for total hip arthroplasty (THA) owing to their inert, hard, and hydrophilic properties (Li *et al.*, 2016). Al_2O_3 also has diverse industrial uses, for example, in catalysts, adsorbents, and gate microelectronic devices (Nmr *et al.*, 2013). Al_2O_3 bio-ceramic (alumina) increases fracture toughness and wear resistance, while maintaining biocompatibility due to its inert nature. It is also able to considerably increase thermal resistance of composites (Imani, 2014).

Al_2O_3 is a hard and relatively cheap material with high hardness, good wear, and corrosion and thermal resistance. It has also high electric resistance, which has

made Al_2O_3 attractive for coating applications where electric insulation and high breakthrough voltage is sought (Matikainen *et al.*, 2014).

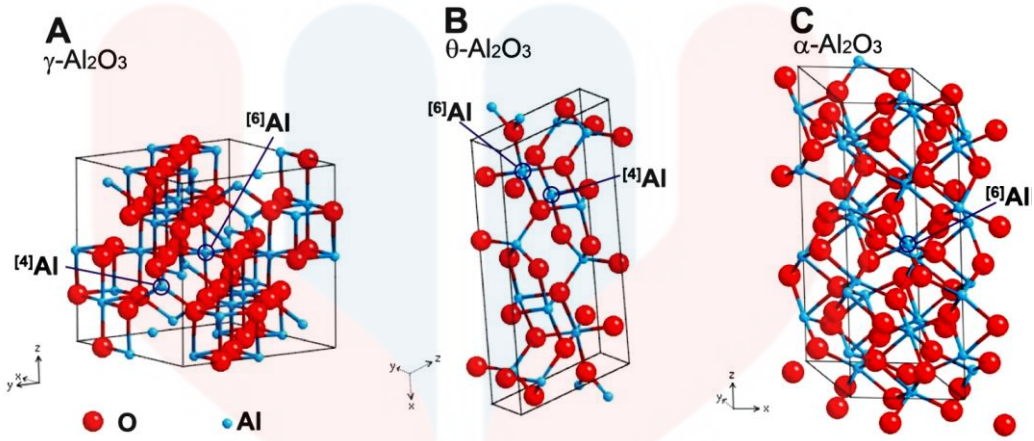

Figure 2.3 : Crystal structure of (A) γ- Al_2O_3, (B) θ- Al_2O_3, and (C) α- Al_2O_3 with crystallographically distinctive aluminum sites (Nmr *et al.*, 2013)

2.4.1 Reinforcement material of alumina-based composite

The purpose of reinforcement is to improve the properties of the material. Different materials of the reinforcement affect the properties of the composites material (Banga *et al.*, 2015). Reinforcement can also enhances the machinability in terms of surface roughness and lower tendency to clog (easier to machine) (Vijayaraghavan, 2007).

Metal reinforcement of CMCs such as s nickel, stainless steel and molybdenum are widely used. The addition of metal reinforcement in composite can decrease residual stress of the ceramic composites and leads to the formation of electrically interconnected skeleton microstructures of metal particles which confer a relatively high electrical conductivity on the composite (Wildan *et al.*, 2002).

As for the polymer reinforcement in CMCs, only fiber components that can withstand the relatively high temperatures required for the production of ceramics, without damage. Other requirements to be met are long-term high-temperature stability, creep resistance, and oxidation stability. Polymeric fiber materials cannot

be used in CMCs because of their degradation at temperatures below 500°C (Clau, 2008).

2.4.2 Application of alumina-based composite

Al_2O_3-based composite such as Al_2O_3-Cr_2O_3 composite manifest excellent potential to be employed for special surface protection of metal components operating at severe working conditions (surface coatings) (Yang *et al.,* 2015). Al_2O_3-based ceramic is also widely use as cutting tools which have a very high abrasion resistance and hot hardness. Chemically they are more stable than high-speed steels and carbides, thus having fewer tendencies to adhere to metals during machining and less tendency to form built-up edge. This result in good surface finish and dimensional accuracy in machining steels (Kumar *et al.,* 2006).

The addition of reinforcement to the Al_2O_3 matrix improved fracture toughness, hardness, strength over the monolithic Al_2O_3 and offered advantages with respect to wear and fracture behaviour when used as cutting tool materials (Jianxin & Xing, 1998). This product is hot pressed to full density and is dark grey in colour as shown in figure 2.4 (Callister, 2011). The structure consists of fine-grained Al_2O_3 with dispersed carbide grains a few microns in diameter. These tools are mainly in high speed machining of cast iron and it shows that they can be applied in a wider range of applications than pure Al_2O_3 because of increased toughness (Trent, 2015). In industrial applications, Al_2O_3 based materials are commonly applied as wear resistant coatings applications (Matikainen *et al.,* 2014). Furthermore, Al_2O_3-based composite can be used as abrasive materials that being used to wear, grind, or cut away other material. Abrasives are used in several forms which is bonded to grinding wheels, as coated abrasives, and as loose grains for example in Figure 2.4.

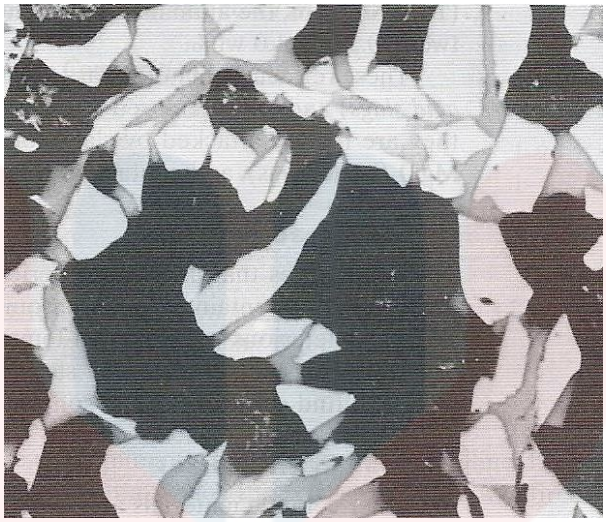

Figure 2.4 : Photomicrograph of an Al_2O_3 bonded ceramic abrasive grains (Callister, 2011)

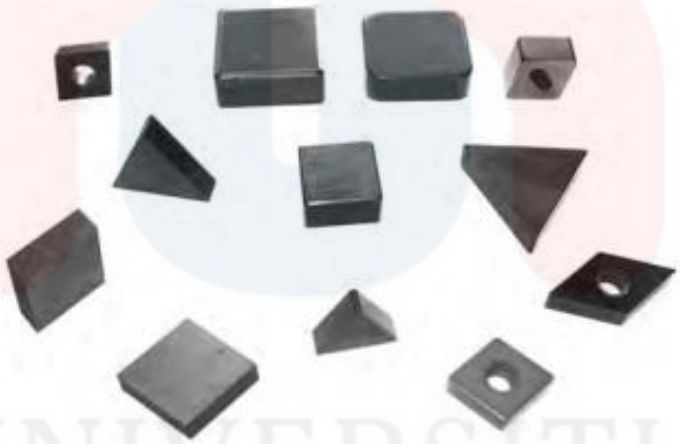

Figure 2.5 : Ceramic cutting material based Al_2O_3 (Zhao, 2014)

2.5 Titania as reinforcement in Al_2O_3

Titania or titanium oxide (TiO_2) can be used as a reinforcing agent due to their excellent properties such as chemical stability in aqueous environments, chemical inertness, and its mechanical resistance. Figure 2.6 shows the side views of stable structures of rutile TiO_2. Ti and O atoms are represented by small grey and big red balls, respectively. Rutile is a mineral composed primarily of TiO_2 and is one of the most used catalysts in chemistry (Wang, 2015)

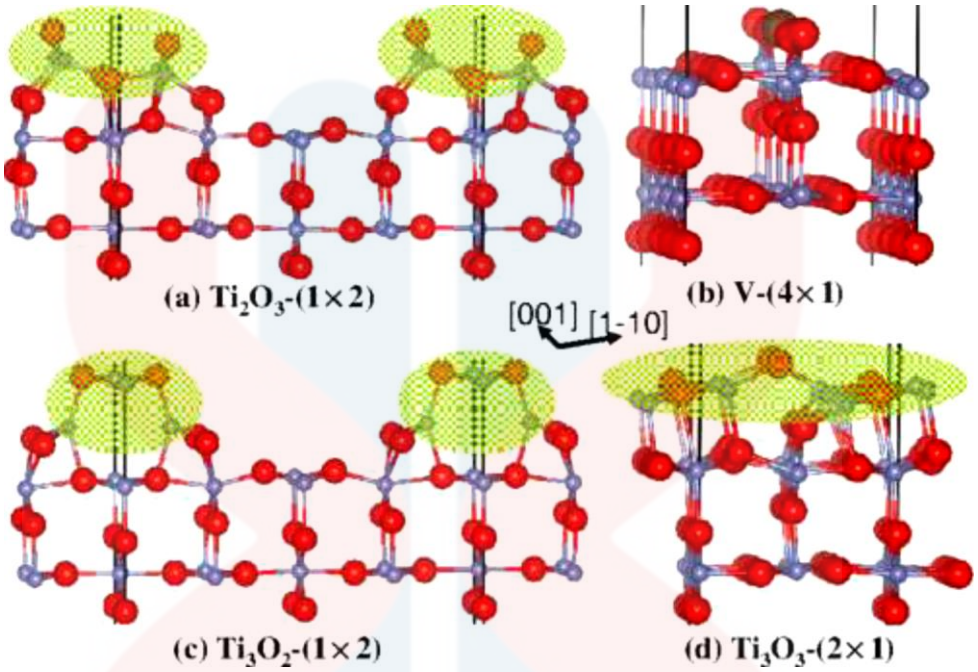

Figure 2.6 : Side views of stable structures of rutile TiO_2 (Wang, 2015).

The addition of TiO_2 has been made to promote densification and retain fine grain size (Trent, 2015). In alumina–tricalcium phosphate–titania composites, the addition of TiO_2 as reinforcement improves the relative density and enhances the rupture strength of the ceramic composites. Also, TiO_2 is well mixed and dispersed in the ceramic matrix and improves the mechanical strength of the composites (Sakka *et al.,* 2014). In other study, the addition of TiO_2 to Al_2O_3 (ceramic matrix) considerably changed its sintering behaviour to manufacture dense ceramics (Bian *et al.*, 2012).

2.6 Alumina-titania composite

Alumina-titania (Al_2O_3-TiO_2) composite is an Al_2O_3-based ceramic (CMC) that are widely used in many areas of industry because of their unique mechanical, electrical, and optical properties (Yang *et al.,* 2008). Al_2O_3-TiO_2 has a high melting point and low coefficient of thermal expansion, which are very useful for

applications that need high temperature condition (Jha *et al.*, 2016). It was reported that addition of titania to alumina considerably changed its sintering behaviour to manufacture dense ceramics (Figure 2.7) (Bian *et al.,* 2012). Increment of TiO_2 content as reinforcement to the Al_2O_3, the relative density of the composites is improved. Also, the addition of TiO_2 can enhance the rupture strength and wear resistance of Al_2O_3 composites (Sakka *et al.,* 2014) (Bian *et al.,* 2012).

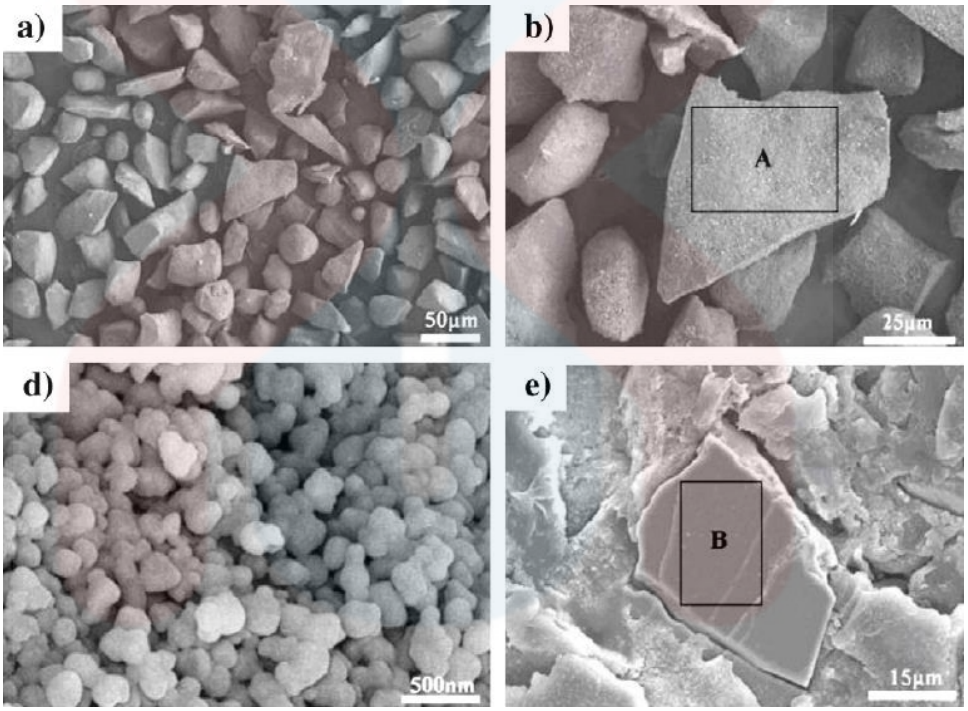

Figure 2.7 : micrographs and EDS analysis of microstructure Al_2O_3-TiO_2 composite powders: (a) overall morphology, (b) morphology of single composite particle, (d) submicron-sized TiO_2 on the surface of Al_2O_3 particle, (e) cross-section morphology of particle (Bian *et al.*, 2012)

2.6.1 Application

Al_2O_3-TiO_2 composites have been widely used as wear resistant coatings in machinery, textile and printing industries due to their high hardness, excellent wear and corrosion, chemical and thermal resistance (Bian *et al.,* 2012). Due to their high melting point and low coefficient of thermal expansion properties is famously used as furnace linings (Jha *et al.,* 2016). Furthermore Al_2O_3-TiO_2 is also used in gas

separation, biomedical processes, support for transition metal catalyst, electronic and optical applications (Bian *et al.,* 2012). Besides that, Al_2O_3-TiO_2 is widely used as thermally-sprayed protective coatings against abrasion, erosion, and cavitation erosion wear, for examples in textile, pulp and paper, and pump industries (Matikainen *et al.*, 2014). In figure 2.8, shows ceramic composite revision ball head and metallic sleeves. These femoral heads have enabled the use of ceramic ball heads in a revision without having to remove the femoral stem (Masson, 2008).

Figure 2.8 : Femoral heads and metallic sleeves (used in medical) (Masson, 2008)

2.7 Processing method of ceramic matrix composite

There are many processing methods to produce CMCs which are chemical vapour deposition, spark plasma sintering, sol-gel method, melt infiltration, polymer impregnation, slurry infiltration/impregnation and powder metallurgy. Since in this research is on preparation of CMCs using powder metallurgy, the discussion on it will be elaborated further in Section 2.8.

2.7.1 Chemical vapour infiltration

Chemical vapour infiltration (CVI) is one of the most attractive industrially available methods to produce fiber - reinforced ceramic matrix composites (CMC). CVI is a process where a porous preform is placed in a surrounding of a reactive gas mixture, which, if thermally activated, decomposes and yields a solid deposit that

fills the pores inside the preform. The main advantages of this technique are the possibility to manufacture complex net or near net shape components at relatively low temperatures, avoiding potential damages of the textile structures, typically used as preform, and to control and modify the microstructure of the matrix. This technique allows the production of strong and tough composites and is ideal to produce composites with characteristics of resistance to corrosion, erosion, and wear. These important features generally overcome the main drawbacks of the CVI process, such as the long manufacturing time of typically some days up to weeks and the run to run reproducibility that in some case still limits the applicability of this technology (Lazzeri, 2016). Figure 2.9 shows the CVI process. The reactant gases, as they flow through the furnace at reduced pressure, diffuse into fibrous preforms, and effluents diffuse back to the preform surface

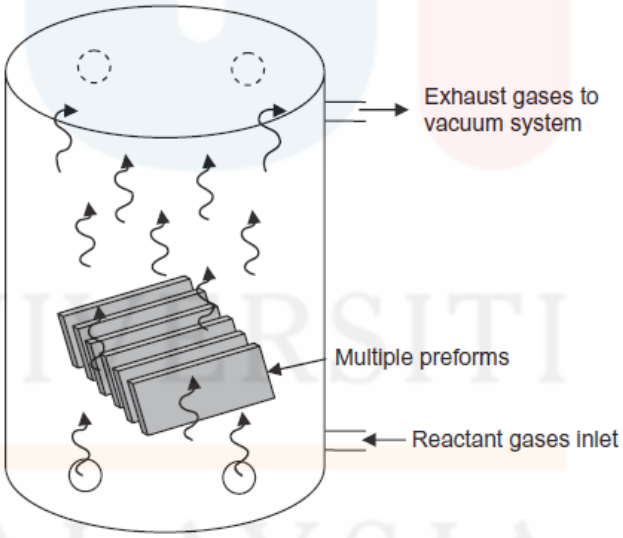

Figure 2.9: CVI process (Lazzeri, 2016).

2.7.2 Sol-gel method

A sol-gel process is described for the preparation of diphasic composite materials. The method involves the growth of extremely fine crystalline or non-crystalline materials inside a pre-made gel structure by soaking the gel in metal

nitrate solution and subsequent precipitation of the metal with the selected anions (using mineral acids) followed by a densification step (Hoffman *et al.,* 1984). Sol-gel synthesis of material is use because it offer several advantages like: low temperature synthesis, ease in controlling composition variations, low cost and potential use in film processing (Somani, 2006). Sol-gel processing involves the use of a hydrolysis reaction to obtain a cross-linked network, which results in the formation of a gel. The gel properties may be controlled by adjusting the pH level, water to metal ratio, and temperature (Kaplan *et al.,* 2006).

2.7.3 Melt infiltration

As for melt infiltration method, it is more suitable for fabrication of highly densified composites. In oxygen containing environment at ultrahigh temperature (over 2000 °C), a dense matrix is of benefit to preventing the oxygen diffusion into the inner of materials. At the same time, there are some unsolved problems in composites fabricated by melt infiltration, such as micro cracks in matrix which may cause poor mechanical and ablation properties (Wang *et al.,* 2016). According to Pi *et al,,* 2012, the composites fabricated from melt infiltration method had excellent ablation resistance. Also, this method outweighs others due to the time-saving preparation and relatively low cost (Chen *et al.,* 2014). Melt infiltration can be used when one of the ceramic matrix elements possesses a relatively low melting point and readily wets the fibres. Ideally, in melt infiltration all available macroscopic porosities for example the porosity between fibre laminates and tows are rapidly filled to yield a dense, uniformly infiltrated composite. Furthermore, components with complex geometries, such as sharp leading edges and rocket engine combustion chambers, can be fabricated easily by this method (Zou *et al.,* 2010).

2.7.4 Polymer impregnation

Polymer impregnation method is optimized to consolidate particulates, and to produce a continuous ceramic network to yield high thermal conductivity monoliths from particulates. Polymer impregnation process consists of impregnating a polymeric precursor into a cast sample or a pressed pellet, pyrolyzing, and crystallizing at high temperature to a final form (Figure 2.11). The use of gas pressure in the polymer impregnation step was found essential to improve the density of the matrix, provided that the nature of the gas and the pressure applied were optimized (Lee *et al.*, 2008). This method also has shown the great advantage of enabling the preparation of high-performance composites. It is feasible to design large-scale components with complex shapes using the Polymer impregnation process (Yin *et al.*, 2015).

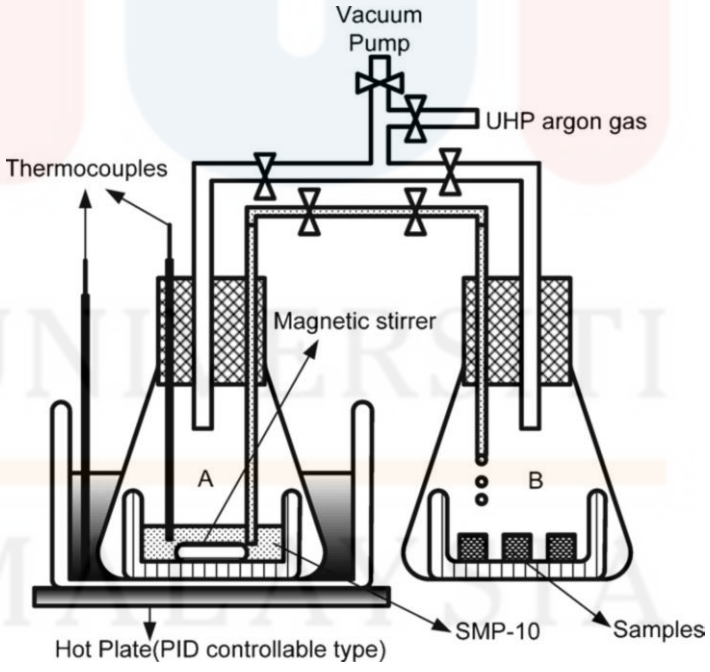

Figure 2.10 : Polymer impregnation system (Lee *et al.*, 2008).

2.7.5 Slurry infiltration/impregnation

Slurry infiltration/impregnation method, the reinforcement is impregnated with a suspension of matrix powder (usually a sol for oxide or oxide or slurry for non-oxide matrix composites). After drying, the material is densified by sintering at high pressure. For non-oxide covalent ceramic powders, such as SiC-powders that display a poor sintering ability, sintering aids (such as oxide mixture forming eutectics) should be added to the slurry. This technique yields composites with almost no residual porosity, high crystallinity and high thermal stability, but it is not suited to the volume production of large parts with complex shape (Krenkel, 2008).

2.8 Powder metallurgy

Powder metallurgy (PM) involves of milling, compaction and sintering. There are several processing method involves in composites. Powder technique is one of the common techniques to produce composites material such as ceramic and metals (Sun *et al.,* 2009). The advantages of PM compare to other techniques are the uniform distribution of reinforcing particles within the matrix and less degradation due to lower processing temperature. PM can be utilised to almost any material that can be process in powder form (Pournaderi *et al., 2012).* P/M can also produce complicated shapes and reduce manufacturing time.

2.8.1 Milling

Milling describes as mechanical agitation that breaks particles into smaller size or agglomerates it; also this process involves mixing two or more powders (Sun *et al.,* 2009). It improves particle distribution which can cause clustering (Corrochano *et al.,* 2011). Mixing of the starting powder or material is an important step in P/M because it controls the distribution of the particles and porosity of the composites and this will influence the behaviours of the final product (Pournaderi *et*

al., 2012). During milling, the forces acting on the material being milled can be impact, attrition, shear and compression.

The main objectives of milling are for the particle size reduction, shape change, agglomeration (putting particle together), mixing or blending two or more material which are not easily mixed and also modification of material properties for example to alter the density or flowability of powders (Angelo, 2012). Milling can be carried out using an industrial high energy mills, medium energy mills and low energy mills. It can be seen that large amount of powders can be processed only at low speed, while small quantity can be processed at higher speed. The milling time decrease with the increase in the energy of the mill (Chang, 2013).

There are several types of mills used for comminution that includes ball mills, vibratory mills, rod mills, and hammer mills (Figure 2.12). Ball mills are the most popular in industry and often used in powder metallurgy for making both powder and powder mixtures. A ball mill consists of a cylindrical vessel rotating horizontally along its axis (Angelo, 2012).

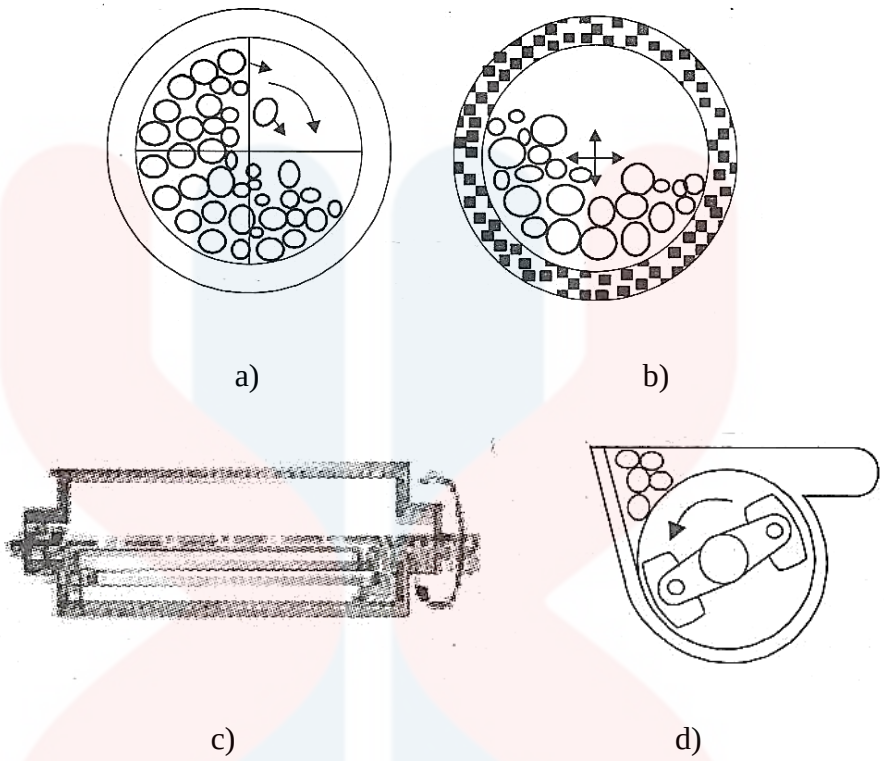

Figure 2.11 : a) Ball mill and b) Vibratory ball mill c) Rodmill and d) Hammer mill (Angelo, 2012)

2.8.2 Compaction

The term 'compaction' is used to describe consolidation of powder particles without the application of heat. The main purpose of compaction is to form metal powder compacts od desired shape with sufficient strength to withstand the ejection from the tools and subsequent handling up to the completion of sintering without breakage or damage (Albdiry & Almosawi, 2011; Angelo, 2012).

Powder compaction techniques can be classified by uniaxial, isotactic (or hydrostatic) and hot pressing. In uniaxial pressing, the powder is compacted in a metal die by pressure that is applied in a single direction, the production rates are high and the process is inexpensive (Figure 2.14). In isotactic pressing, the powdered material is obtained in a rubber envelope and the pressure is applied by a fluid, isotatically. More complicated shapes are possible than uniaxial however it is more time consuming and expensive.

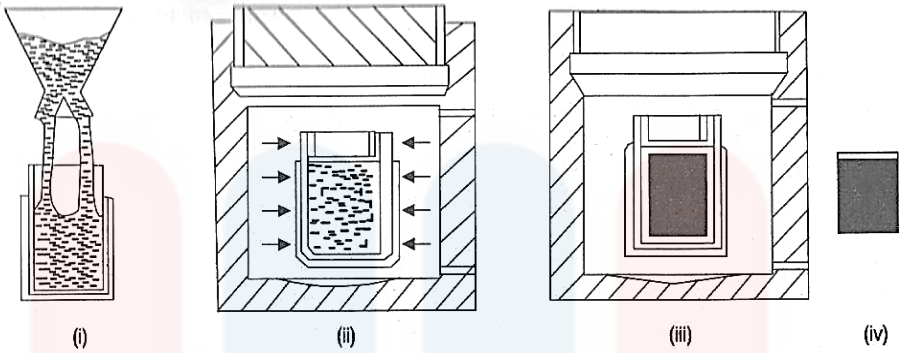

Figure 2.12 : Steps in cold isotactic pressing : i) mould filling ii) pressurizing the mould iii) depressurizing iv) green part (Angelo, 2012)

Hot pressing refers to the process which pressure is applied to the powder at elevated temperatures (Callister, 2011). This can be carried out by hot pressing, hot extrusion, hot rolling and Hot Isotactic Pressing (HIP) (Angelo, 2012). This is an expensive fabrication technique that has some limitations which is costly in term of time (Callister, 2011).

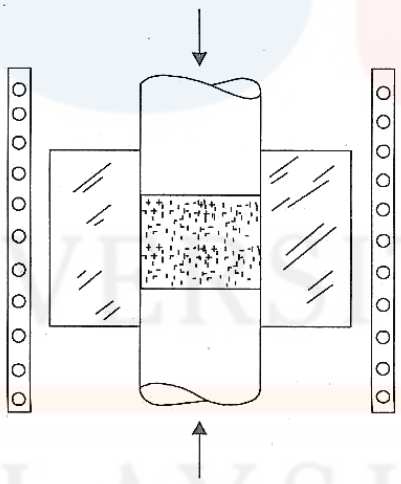

Figure 2.13 : Uniaxial hot pressing unit (Angelo, 2012)

Lubricants in die compaction is necessary due to the presence of frictional forces limits the degree of densification. Lubricant can minimize the frictional forces

encountered during compaction. Lubricants are normally organic compounds or metallic stearate (Angelo, 2012).

There are three stages involves in compacting process, the first stage consist of packing the particles together (without deformation), second stage is plastic deformation and cold working followed by bulk compression that involves in fracture, fragmentation, or brittle powders (Figure 2.15) (Albdiry & Almosawi, 2011). The most widely used method is the conventional uniaxial powder compaction, with the applied pressure along one axis using hard tooling of die and punches (Sun *et al.*, 2009).

If the compaction is increased the powder distribution of powder becomes narrower and the particles almost completely broken down which caused by high stress. The conclusion from this study is the higher pressure results in a finer and homogeneous microstructure (Garg *et al.*, 2007). On the other hand, large amount of porosity is observed at a lower pressure compare with the porosity at the higher compaction pressure (Mahani, 2013).

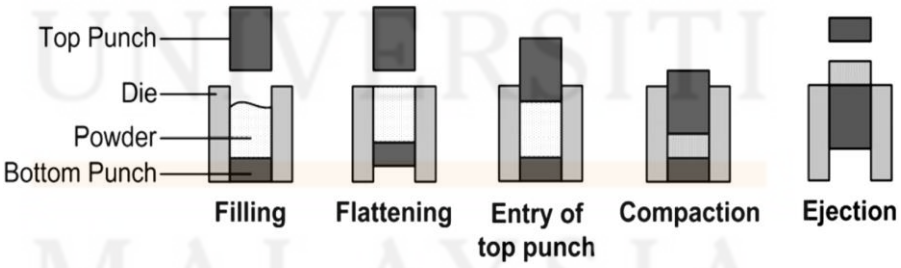

Figure 2.14 : The progression of motions for uniaxial die compaction (Sun *et al.*, 2009)

Density of the sintered parts is easy to adjust by regulating the processing variables such as compacting pressure (Wang, 2007). With the increase of applied pressure, the density of the composites increases with the decrease of the porosity.

Densification is inhibit because extra deformation is needed in the soft particles to fill the voids between the contact particles (Abdoli *et al.,* 2008). In other study, high compaction pressure will results in the increase of green and sintered density. This is due to the particle to particle contact and increase the amount of cold work which leads to the densification (Hadas *et al.,* 2011).

2.8.3 Sintering

Sintering defines as the thermal treatment of a powder or a compact for the purpose of increasing strength by bonding together of the particles (Angelo, 2012) (Albdiry & Almosawi, 2011). It can occur at temperatures below the melting point by solid-state atomic transport phenomenon so that the liquid phase is normally not present (Sun *et al.,* 2009; Callister, 2011).

During the initial sintering stage, necks form along the contact regions between adjacent particles, in addition the grain boundary forms along each neck, and every interstice between particles becomes a pore. As sintering progresses, the pores becomes smaller and more spherical in shape as shown in the figure 2.16 (Callister, 2011).

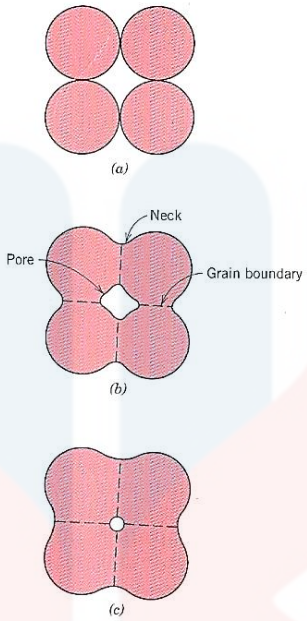

Figure 2.15 : (a) Powder particles after pressing (b) Particles coalescence and pore formation (c) The pores change size and shape (Callister, 2011)

The compact is usually heated in a protective atmosphere such as argon or hydrogen. Several changes occur during sintering like shrinkage, formation of solid solution, and development of the final microstructure. Usually, sintering resulted in reduction or elimination of porosity leading to densification. There are several types of sintering which are solid state, liquid phase sintering, activated sintering, reaction sintering, rate controlled sintering, microwave sintering, self-propagating high-temperature synthesis, gas plasma sintering and spark plasma sintering (Angelo, 2012).

CHAPTER 3

MATERIALS AND METHOD

3.1 Introduction

This chapter explains the materials and experimental work involved in this research. The step in this study can be presented in Fig 3.1. This research involves of two stages which are preparation and characterization of the composite. Overall flowchart for this research is shown in Figure 3.1.

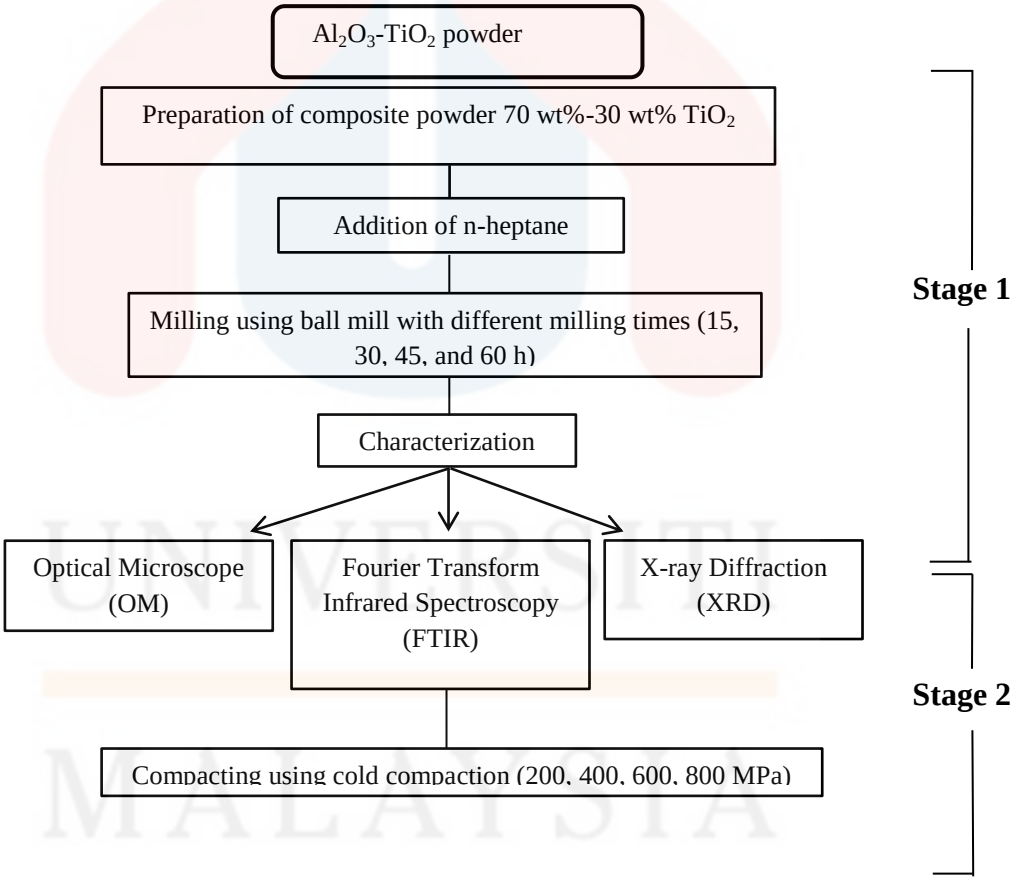

Stage 1 : Material Preparation
Stage 2 : Material Analysis

Figure 3.1 : Overall experiments in this research

3.2 Raw Materials

Al_2O_3 powder and TiO_2 powder are the material that was being used in this experiment. Al_2O_3 (> 99.9% purity, average particle size > 20 μm), anatase TiO_2 (> 99.5% purity, average particle size >21 nm) was used in the study and were purchased from Sigma Aldrich.

3.3 Composite preparation

Al_2O_3–TiO_2 composite was fabricated using powder metallurgy method. The composition of 70 wt%-30 wt.% titania mixture was used and was calculated using rule of mixture.

3.3.1 Milling

Before milling, n-heptane was added to powder mixture to ensure that the powder . Then, the powder mixture was milled using low energy ball milling (Figure 3.2) with different milling times (15 h, 30 h, 45 h, 60 h). Alumina ball with 10mm diameter with 10:1 ball mill powder ratio was used and 100 rpm milling speed.

Figure 3.2 : Low energy ball milling

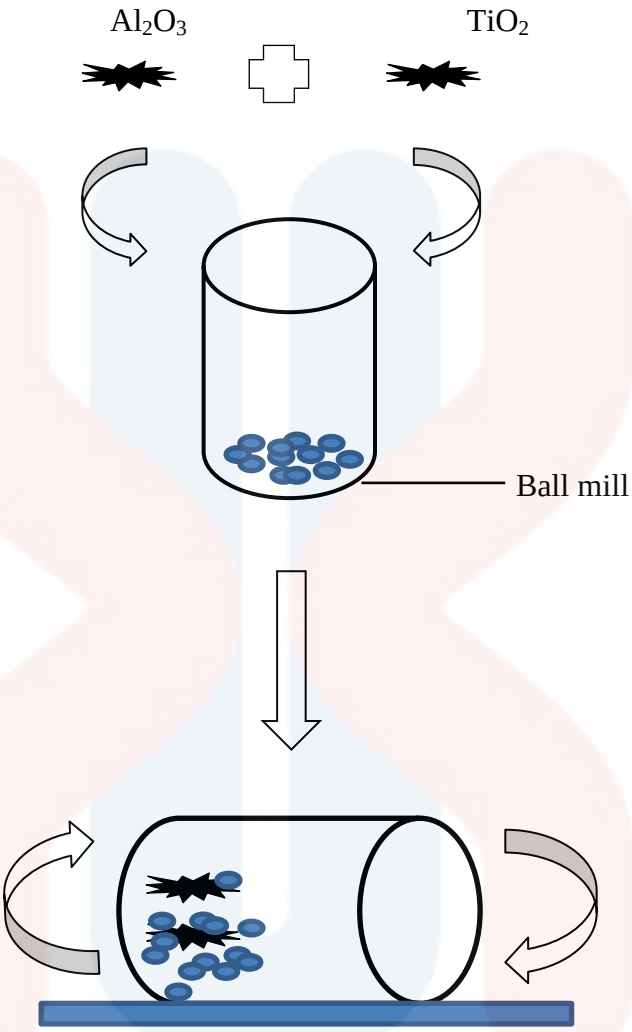

Figure 3.3 : Process of milling

3.3.2 Cold compaction

Prior to compaction, the mixture was mixed with zinc stearate to increase powder compressibility during compaction. The composite was then compacted using uniaxial single action hydraulic press (Figure 3.4) using stainless steel die at different pressures (200, 400, 600, 800 MPa).

Figure 3.4 : Hand press

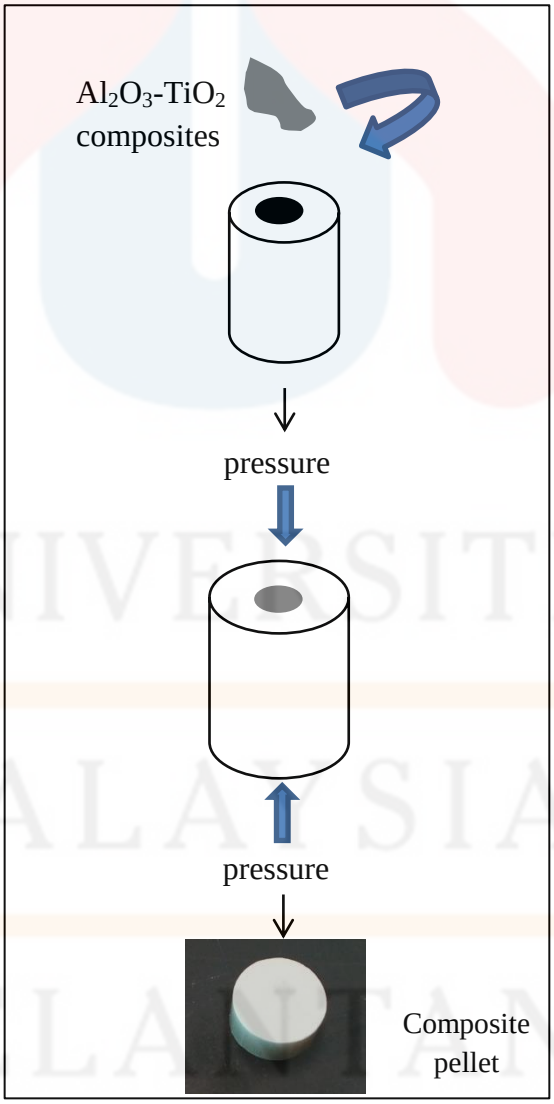

Figure 3.5 : Al_2O_3-TiO_2 composites during compaction

3.4 Composite characterization

Composite that was characterized in this study was phase analysis, surface area analysis, microstructure and density and porosity measurement.

3.4.1 Phase analysis

The Al_2O_3-TiO_2 nanocomposite was characterized for its phase identification using XRD. This was perform using Bruker D2 Phaser with Cu Kα radiation (λ = 0.154 nm). The step size was fixed at 0.02° with the 2θ angle of 10° to 90°. Software DIFFRAC.EVA phase identification of X- Ray diffraction pattern was used to perform qualitative and quantitive analysis of the composite. The information from qualitative information was used to determine crystallize size and internal strain. WH is the most common method used to evaluate the crystallite size and internal strain in powders. The assumption is that the whole line broadening, B_o is a sum of the total broadening of size, lattice strain and instrument (Cullity and Stock, 2001):

$$B_o = B_i - B_{crys} + B_{strain} \quad \text{Eq.1}$$

Where B_i broadening due to instrumental, B_{cryst} broadening due to size and Bs_{train} broadening due to strain. Subtracting the instrumental effect, Eq. 2 (Cullity and Stock, 2001) becomes:

$$B_r = B_{crys} + B_{strain} \quad \text{Eq.2}$$

Where Br represent the overall broadening after eliminating the instrument broadening. Therefore, due to crystallite size and internal strain, WH method is given by (Williamson and Hall, 1953):

$$B_r \cos\theta = \frac{k\lambda}{D} + \eta \sin\theta \quad \text{Eq.3}$$

Where η is internal strain B is crystalline size, λ is the wavelength of the X-Ray used (1.5406 A^o), θ is the Bragg angle, k is a constant and L can obtained from observed

full width at half maximum (FWHM) by convoluting Gaussian profile which sample broadening. Only three Al_2O_3 Bragg's peaks of [-1,1,4] and [-2,1,0] reflections were considered for calculating Al_2O_3 crystallite size and internal strain since they are the most highest and have the closest match from XRD database. The slope is plot either in positive or negative sides indicates the connection whether the sample in stress or stress-free state. Since the [-1,1,4] and [-2,1,0] reflections were derived from the same crystallite therefore, a straight line was drawn, according to the data points

3.4.2 Fourier Transform Infrared Spectroscopy

The infrared spectrum of powder mixture composites were analyse using Fourier Transform Infrared Spectroscopy. The functional group of each composite was determined together with the wavenumber. In addition**,** Fourier transform infrared (FTIR) spectrometer was used to determine the adsorption of organic molecules in raw materials and nanocomposite. FTIR spectra was evaluated using Thermo Scientific^{TM} iD7 with single-bounce attenuated total reflectance (ATR) technique. The FTIR spectra were recorded in the scanning range of 400–4,000 cm^{-1} at 4 cm^{-1} with 16 scans. The analysis of infrared spectra on the raw materials and nanocomposite were done using OMNIC spectra software.

3.4.3 Microstructure

The morphology of the composites was examined by Optical microscopy (OM). The specimens were examined under 20x magnifications for every milled time.

3.4.4 Density and porosity measurement

After compaction, the dimension and mass of composite were measured. This information was used to calculate green density using general calculation of green density, GD as follows (Eq.4):

$$GD = \frac{m}{V} \qquad \text{Eq.4}$$

where m is mass and V is volume.

In order to study the compressibility of produced composite, densification parameter were calculated. Densification parameter was determined using Eq. 5:

$$\text{Density} = \frac{GD - AD}{TD - AD} \qquad \text{Eq.5}$$

where AD is apparent density and TD is theoritical density.

CHAPTER 4

RESULTS AND DISCUSSION

4.1 X-ray Diffraction

X-ray diffraction (XRD) was used to identify the structural properties of milled Al_2O_3-TiO_2 powders. Diffract.Eva software was used to find the matches pattern of Al_2O_3 and TiO_2 powders. The information gathered from the peak pattern also used to calculate crystallite size and internal strain.

4.1.1 Phase Identification

XRD patterns of the powder mixture of Al_2O_3-TiO_2 composites powder mixtures after milled at 15h, 30h, 45h and 60h are shown in the Figure 4.1. The peak positions are almost identical for all milling times. However, the intensity of Al_2O_3 located at 77º shows slightly different from the other milling time. The peak-height appears to decrease with further increased of milling time. 2θ at 63.2º of TiO_2 is also reduced as milling time increased, and the peak is diminishing at 60 h of milling. There was no visible new phase formation and the peak of the powder mixture does not show any shift either to the left or right thus it is assumed that there is no expansion or reduction of lattice parameter occurred. This is caused by the low energy milling which generate less energy to change the internal structure of the composite. The highest intensity of composite powder mixture in Figure 4.1 was located at 35.5º which identified as Al_2O_3 crystalline.

The broadening of the peak was decreased as the milling time increased. It can be clearly seen the broadened peak of Al_2O_3 located at 35.5º and 57.5º. This indicated that there is difference in the area of the peak. The broadening of composite

powder mixture is attributed from the refinement of structure which can be contributed from the changes in crystallite size and internal strain.

Apart from that, the peak located at 25º and 26º, 37.5º and 38º of the mixture powder seems to overlap because both peaks are very close to each other. The reduction of the peaks intensity is more obvious in TiO_2 compared to Al_2O_3 due to the size of TiO_2 was smaller than Al_2O_3 matrix.

The XRD patterns of raw Al_2O_3 and TiO_2 particles are also shown in figure 4.1. It shows the absence of spurious diffraction, which proves the crystallographic purity (Nassar *et al.*, 2015). The peaks of composite powder mixture were not shifted from the pure powder. There was no broadening of milled mixture compared to the starting powder. However, the main diffraction peak of Al_2O_3 milled powder located at 35.5º slightly reduced in intensity compared with Al_2O_3 pure powder. The TiO_2 peak was shortened and diminished as the milling time increased which can be explained by the diffusion of TiO_2 into Al_2O_3 matrix.

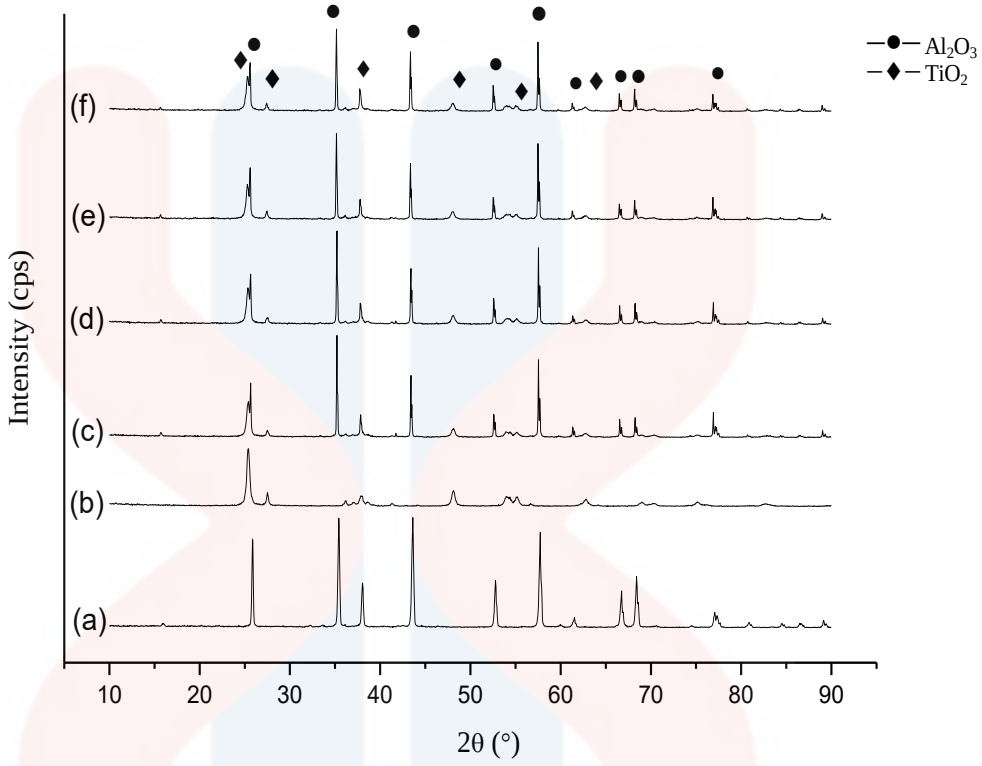

Figure 4.1 : Phase identification for (a) Al_2O_3 (b) TiO_2 ; Al_2O_3-TiO_2 milled at (c) 15 h (d) 30 h (e) 45 h (f) 60 h

4.1.2 Crystallite Size and Internal Strain

The data derived from WH method were plot $B_r \cos\theta$ against $\sin\theta$ is plotted as shown in figure below. The crystallite size was calculated from y intercept while internal strain was extracted from the slope. Based on the graph, all of the intercept and slope is positive value indicates that the milling time was decreased. The plot shows linear indicating that the structure refinement was not only originated from crystallite size but also the internal strain.

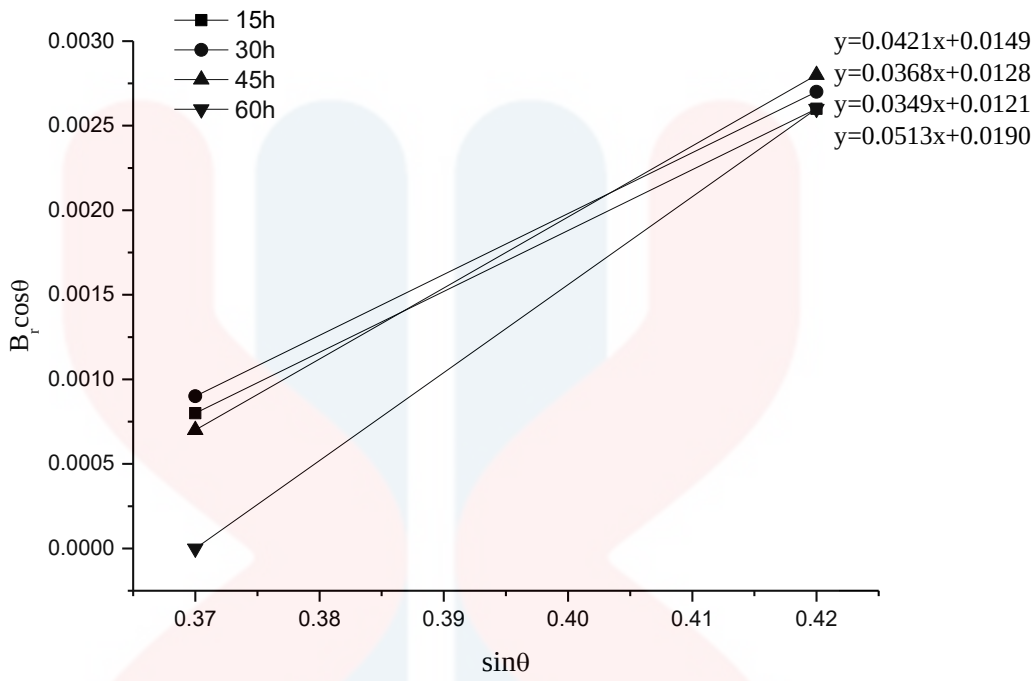

Figure 4.2 : Plot *of* $B_r cos\,\theta$ against $sin\,\theta$ for calculating crystallite size and internal strain for different powder milled.

Crystallite size was calculated from Williamson-Hall equation, and the graph was plotted against different milling time as shown in Figure 4.2. It is shown that the Al_2O_3 crystallite size reduce significantly as the milling time increase from 15 h to 60 h. This is because the higher milling time cause a longer collision between powder particle and the wall of the milling container. This collision causes the grain size to reduce as the milling time increase.

Figure 4.2 also showed that the internal strain was increased as the crystallite size decreased. The lattice strain generally follows the features of dislocation density, it increases as the grain size decreased (Chouket *et al.*, 2016). The internal strain was induced by the ball mill that gave an impact to the powder and the container. Furthermore, the increase in the lattice strain indicates the strain hardening of the powders due to ball-milling (Ogawa *et al.*, 2015).

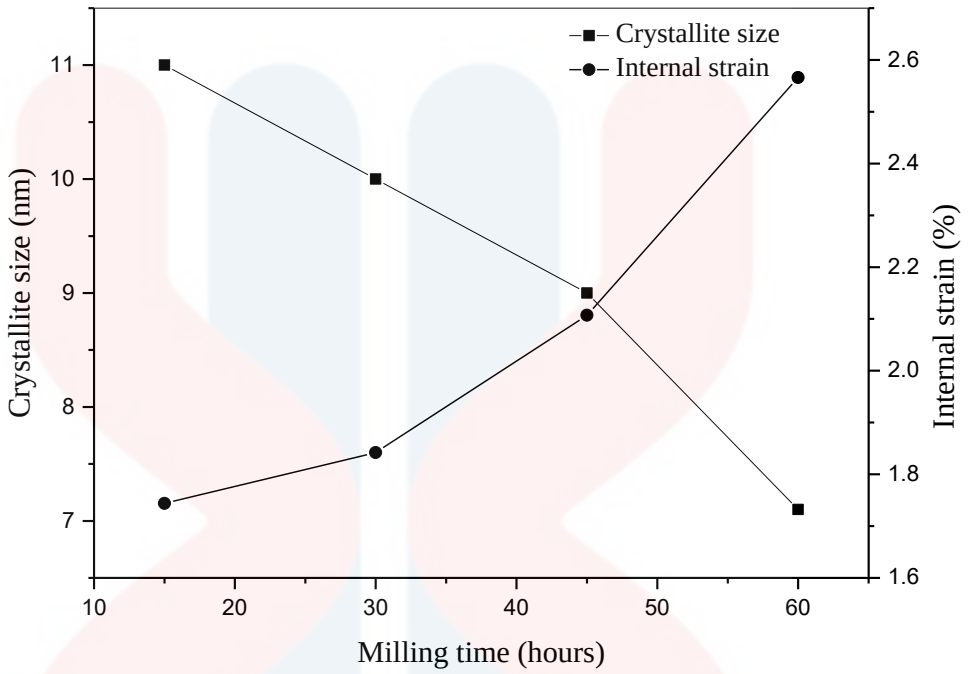

Figure 4.3 : Crystallite size and internal strain of Al_2O_3 of as milled powder with different milling time

4.2 Microstructure of as milled powder

Microstructure of the pure powder before milled, was captured under Optical microscope (OM) as shown in Figure 4.4. Different size of the powder particle can be seen. The particle size of TiO_2 is smaller with large surface area compared to that of Al_2O_3 particles. Figure 4.4 also shows the OM micrographs of as-milled Al_2O_3-TiO_2 powder at different milling time. The particle distributions were uniformly distributed in all milling times with irregular shape. The sizes of powder particles were decreased and well distributed with the increase of milling time. However, the difference in the size of the particle was not that significant. The reason is due to not enough energy to initiate deformation of composite powder mixture. Nevertheless, it is obvious that the particle size was finer and well distributed when milled at 60 h indicating that milling at this time produced higher impact energy.

It can be concluded that the increased in milling time caused the decreased in particle size with uniform particles distribution.

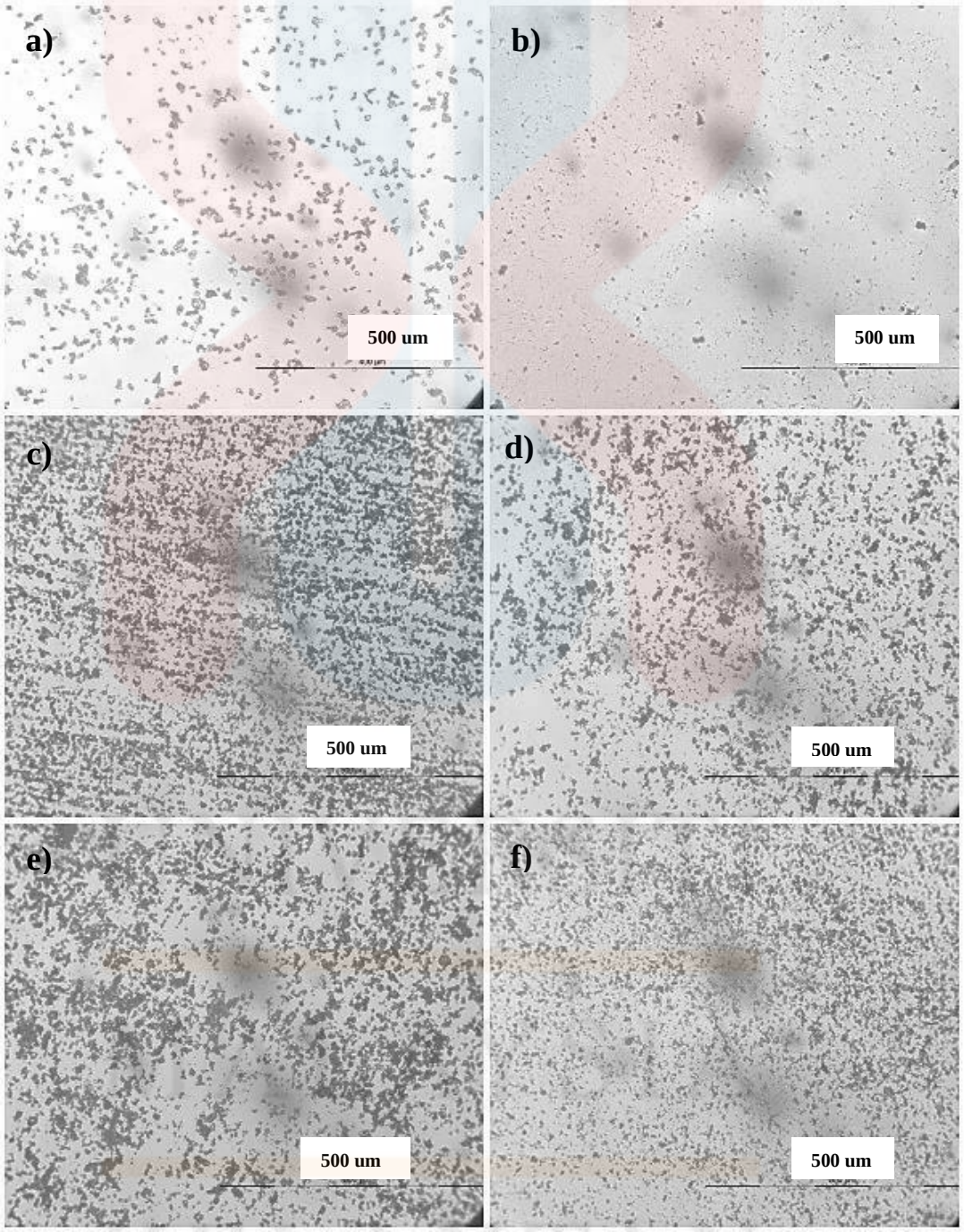

Figure 4.4 : OM images of powder a) Al_2O_3 b) TiO_2 and powder mixture composite milled at c) 15 h d) 30 h e) 45 h f) 60 h

4.3 Properties of Al_2O_3-TiO_2 Composite

After the milling process, Al_2O_3-TiO_2 nanocomposiote powder were compacted using uniaxial single action hydraulic press using stainless steel die at different pressure. Then the density and densification parameter of the composite were calculated.

4.3.1 Green Density

Densities of Al_2O_3-TiO_2 powder compact were plotted against different compaction pressure are shown in Figure 4.3. It was found that the increased in compaction pressure from 200 MPa to 800 MPa, increased the GD. Uniaxial compaction process can be described as having three stages which are rearrangement, plastic deformation, and mechanical interlocking of powder particles. Particle rearrangement occurs to fill the large gaps between particles. However, only rearrangement stages present in this composites without plastic deformation which will further increasing the GD (Wang *et al.,* 2015).

GD is continually increases from 2.637 g/cm^3 at 200 MPa to 2.98 g/cm^3 at 800 MPa. The increase of GD can be due to several factors such as particle size distribution, and the morphology of the powder compact. According to Park *et al.*, 2012, the increased in compaction lead to a higher in GD due to the inter powder holes or gaps were diminished. Besides, the increment in GD was also attributed from the increased in particle-particle contact and assist in amount of cold work which causes lower porosity generation as the compaction pressure increased. Thus, lead to denser composite (Hadas *et al.,* 2011).

Furthermore, GD of the composite was increased as the milling time increased. During compaction, the composite were easily compressed as the milling

time increased, induced smaller particle size. This can be explained by the small size of particle. According to Wang *et al.,* 2008, the smaller the particle sizes, the higher the GD. This is because the fine particles are easily filled into pores among coarse particles leading to the reduced porosity and leading to increase in green density.

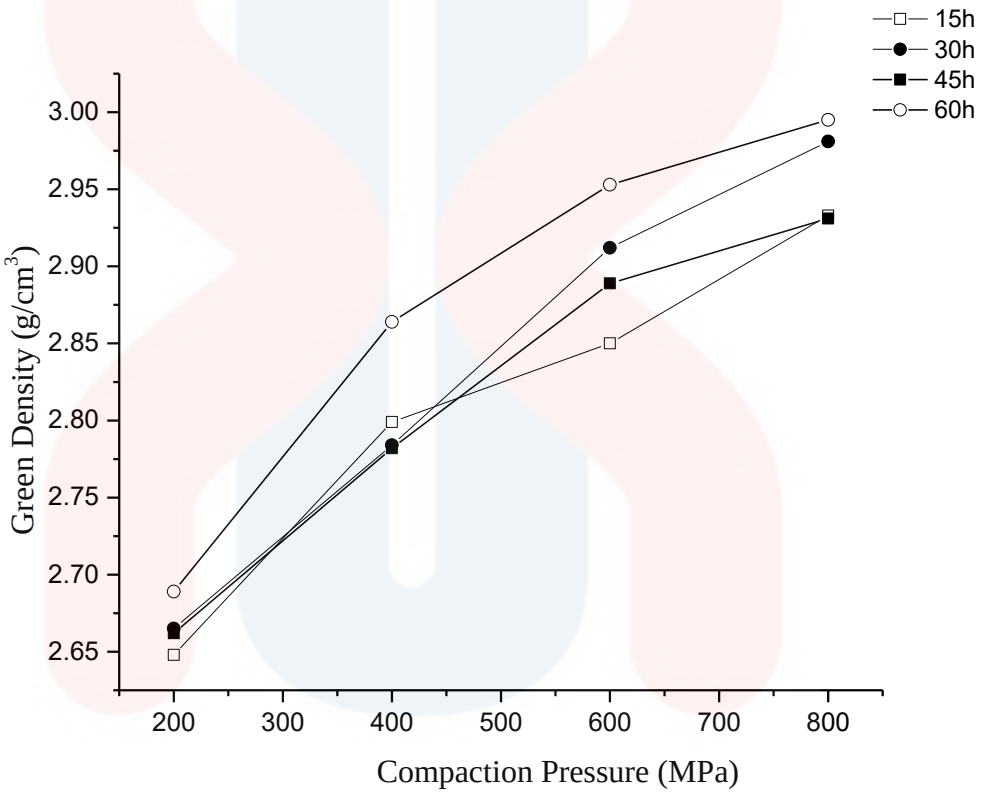

Figure 4.5 : Green density of composite powder at different milling time and different compaction pressure

4.3.2 Densification Parameter

Densification parameters of Al_2O_3-TiO_2 powder composites plotted against different compaction pressure is shown in Fig. 4.6. It is found that the densification parameter of Al_2O_3-TiO_2 increased with the increased compaction pressure. This can be explained by the particle size distribution and the porosity of the composites with

different compaction pressure and different milling time. When compared between Figures 4.5 and 4.6, it proof that GD reflects the densification of the composite.

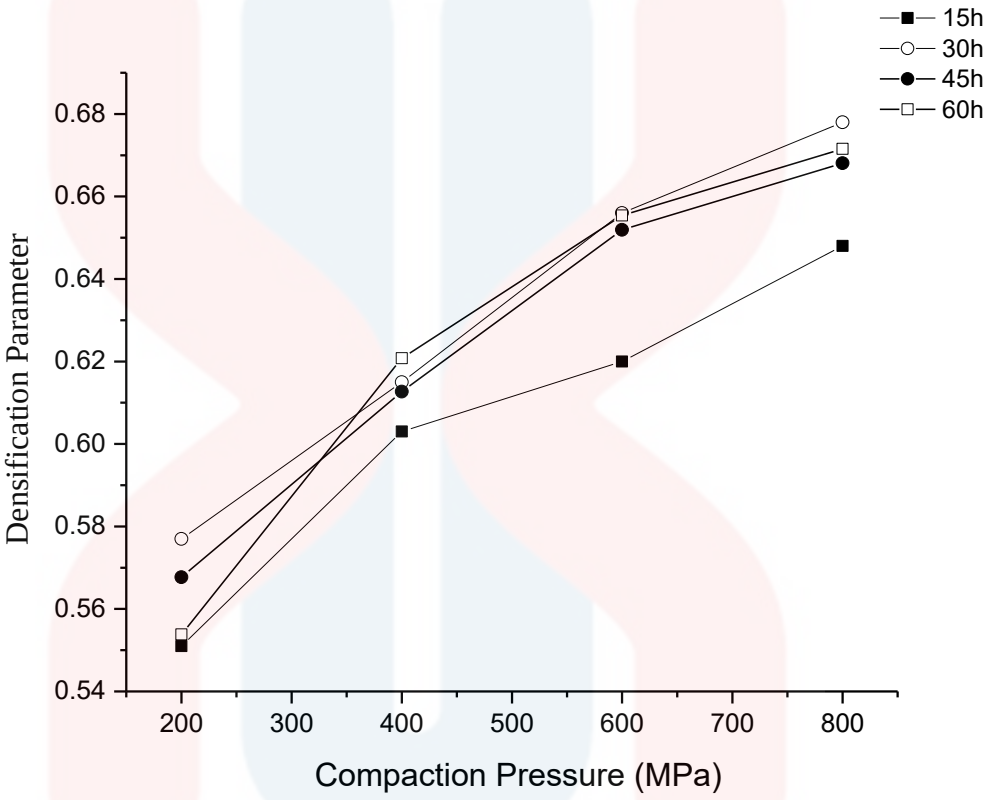

Figure 4.6 : Densification parameter of powder with different milling time against different compaction pressure

In order to relate compaction pressure and relative density or porosity for the composites, the Panelli & Ambrozio Filho, 2001 equation was used:

$$\ln\left[\frac{1}{1-D}\right] = AP^{1/2} + B \qquad \text{Eq. 6}$$

where D is densification parameter, A is the slope of the graph which represents the plastic deformation, P is compaction pressure and B is the intercept of the plot. The plot observed indicates that there plastic deformation in all milling time. In Figure 4.7 the high values of A are achieved when the milled time of the powder is increase. This may be due to the size of the powder is smaller with the increased in milling

time. In addition, the increased of compaction pressure also led to the increase of plastic deformation, possibly due to the higher densities.

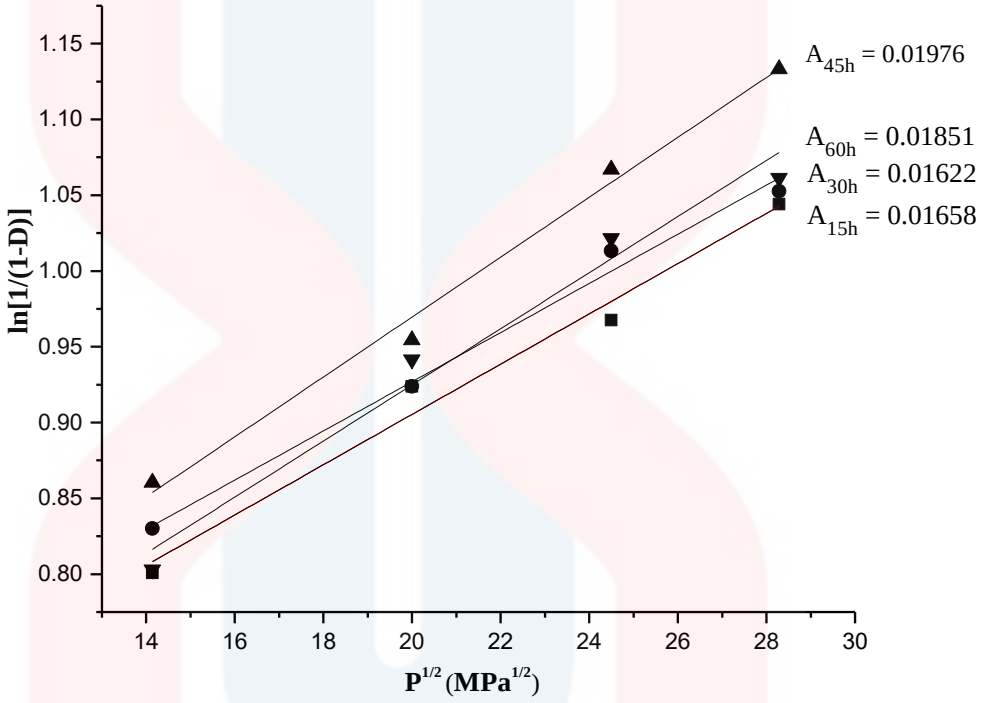

Figure 4.7 : Plot of experimental data for green compact using the equation produced by Panelli and Ambrozio Filho (1998)

4.4 FTIR Analysis

The result obtained from FTIR is shown in Figure 4.8 and Figure 4.9. In Figure 4.8, it was observed that there was no functional group obtained for starting powders, Al_2O_3. However, there was aliphatic hydrocarbon and olefins present in the starting powders of TiO_2. The broad and intense peak was located at 2925.38 for aliphatic hydrocarbons group at 2650 wavenumber and 3289.52 and 1647.95 for olefins group at 3500 and 1500 wavenumber.

Figure 4.8 shows the composite powder mixture of all milling times. The functional group that present in all milling time was aliphatic hydrocarbons. Small olefins peak was left and diminished after milled for 15, 30, 45, and 60 h. There were only three aliphatic bond between Al_2O_3 matrix and TiO_2 reinforcement that were remained in the composite powder mixture due to the low energy milling. The energy was insufficient to induce bonding in the composite.

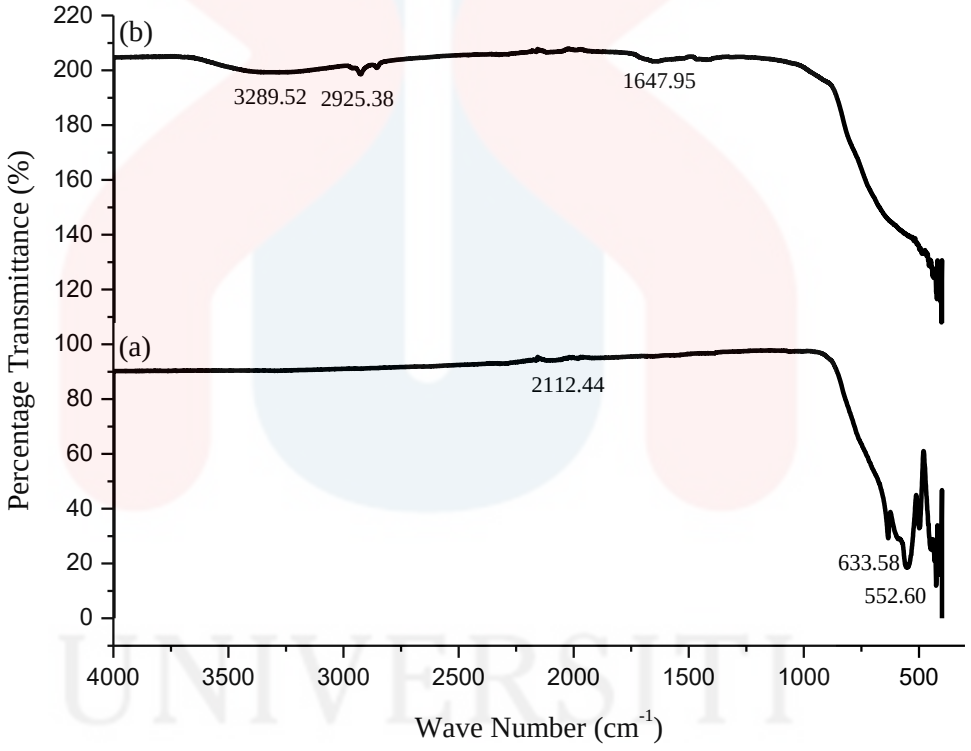

Figure 4.8 : FTIR spectra of starting powders (a) Al_2O_3 (b) TiO_2

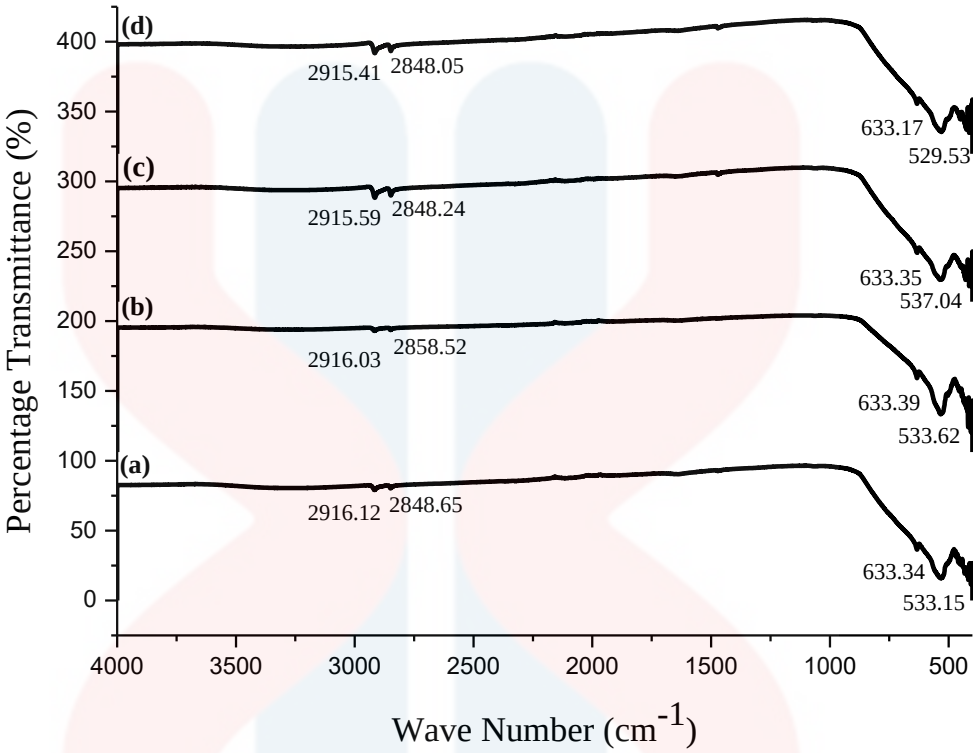

Figure 4.9 : FTIR spectra of powder mixture Al_2O_3-TiO_2 composites at milling time (a) 15 h (b) 30 h (c) 45 h (d) 60 h

CHAPTER 5

CONCLUSION

5.1 Conclusion

In this research, the Al_2O_3- TiO_2 composites prepared by powder metallurgy method have been achieved. First step was milling, which was carried out by milled pure Al_2O_3 and TiO_2 powder with low energy milling of 15, 30, 45 and 60 h. Bulk composites was achieved by compaction under different pressure of 200, 400, 600, and 800 MPa. There are several conclusions drawn from this study which are :

1. The bulk composite that was produced at 800 MPa has the best properties, which possessed high densification parameter due to the low porosity in microstructure.
2. Powder mixture composite that was milled for 60h was easily compact compare to other due the small in particle size.
3. The optimum compaction pressure and milling time is 800 MPa and 60h of milled which is the optimum parameter for Al_2O_3- TiO_2 composites.
4. The changes in this study, the morphology and particle size are not significantly change due to low energy milling.

5.2 Suggestion for future work

From this research, by producing bulk composite using PM method, only the size of the powder and the particle distribution was observed under OM. It is suggested that in the future by using SEM instead of OM to observe the powder morphology so that the microstructure and size is observed and study in detail and precise.

The low energy milling can be replaced with high energy milling and mill in a longer time so that the effect is more obvious. By using high energy mill, the size and morphology of the powder will change significantly and probably induced new phase formation.

Other than that, after compaction, the bulk composite is suggested to be sintered to achieve a better microstructure with clear porosity and defect. The density and hardness of the composite will also be increase after sintering process.

Reference

Aigbodion, V. S., Agunsoye, J. O., Kalu, V., Asuke, F., Ola, S., Metallurgical, N., & Centre, D. (2010). Microstructure and Mechanical Properties of Ceramic Composites. *Minarels and Materials Characterization and Engineering*, *9*(6), 527–538.

Albdiry, M. T., & Almosawi, A. I. (2011). Effect of compacting pressure on microstructure and mechanical properties of carbide cutting tools, *54*(5), 585–591.

Auerkari, P. (1996). Mechanical and physical properties of engineering alumina ceramics. *Technical Research Centre of Finland*, *1792*, 26.

Banga, H., Singh, V. K., & Choudhary, S. K. (2015). Fabrication and Study of Mechanical Properties of Bamboo Fibre Reinforced Bio-Composites. *Innovative Systems Design and Engineering*, *6*(1), 84–99.

Bian, H., Yang, Y., Wang, Y., & Tian, W. (2012). Preparation of nanostructured alumina – titania composite powders by spray drying , heat treatment and plasma treatment. *Powder Technology*, *219*, 257–263.

Chen, S., Zhang, C., Zhang, Y., & Hu, H. (2014). Composites : Part B Preparation and properties of carbon fiber reinforced ZrC – ZrB 2 based composites via reactive melt infiltration. *Composites: Part B*, *60*, 222–226.

Chouket, A., Cheikhrouhou-Koubaa, W., Cheikhrouhou, A., Optasanu, V., Bidault, O., & Khitouni, M. (2016). Structural, microstructural and dielectric studies in multiferroic LaSrNiO4-δ prepared by mechanical milling method. *Journal of Alloys and Compounds*, *662*, 467–474.

Clau, B. (2008). Fibers for Ceramic Matrix Composites, 1–20.

Corrochano, J., Lieblich, M., & Ibáñez, J. (2011). Composites : Part A The effect of ball milling on the microstructure of powder metallurgy aluminium matrix composites reinforced with MoSi 2 intermetallic particles. *Composites Part A*, *42*(9), 1093–1099.

Ding, D. (2014). *Processing, properties and applications of ceramic matrix composites, SiCf/SiC: an overview*. *Advances in ceramic matrix composites*. Woodhead Publishing Limited.

Furlani, E., Aneggi, E., Leitenburg, C. De, & Maschio, S. (2014). High energy ball milling of titania and titania – ceria powder mixtures. *Powder Technology*, *254*, 591–596.

Gutmanas, E. Y., & Gotman, I. (1999). Dense High-temperature Ceramics by Thermal Explosion Under Pressure. *Europian Ceramic Society*, *19*.

Hadas, S., Annamalai, A. R., & Upadhyaya, A. (2011). Effect of compaction pressure and tempering on densification , microstructural evolution , mechanical

properties , wear and machinability response of sinter hardened Ancorsteel 4300 – 0 ? 6Gr, *26*(5), 263–270.

Hoffman, D. (1984). Diphasic Ceramic Composite Via a Sol-Gel Method, *2*(3), 245–247.

Huang, J., & Nayak, P. K. (2014). *Strengthening alumina ceramic matrix nanocomposites using spark plasma sintering*. *Advances in ceramic matrix composites*. Woodhead Publishing Limited.

Imani, R. (2014). Characterization of a novel nanobiomaterial fabricated from HA , TiO 2 and Al 2 O 3 powders : an in vitro study.

Isaac Chang, Y. Z. (2013). *Advances in powder metallurgy*.

J. G. Sun, C. M. Deemer, W. A. Ellingson, J. W. (1989). NDE Technologies for Ceramic Matrix Composites: Oxide and Non-Oxide, (Cvi), 1–18.

Jha, S. K., Lebrun, J. M., & Raj, R. (2016). Journal of the European Ceramic Society Phase transformation in the alumina – titania system during flash sintering experiments. *Europian Ceramic Society*, *36*, 733–739.

Jianxin, D., & Xing, A. (1998). Wear behavior and mechanisms of alumina-based ceramic tools in machining of ferrous and non-. *Tribology International*, *30*(11), 807–813.

Krenkel, W. (2008). *Ceramic Matrix Composites: Fiber Reinforced Ceramics and Their Applications*.

Kuhn, H. (2012). *Powder metallurgy processing*.

Kumar, A. S., Durai, A. R., & Sornakumar, T. (2006). Wear behaviour of alumina based ceramic cutting tools on machining steels. *Tribology International*, *39*, 191–197.

Kumar, S., Ramanathan, S., & Sundarrajan, S. (2015). Synthesis , microstructural and mechanical properties of ex situ zircon particles (ZrSiO 4) reinforced Metal Matrix Composites (MMCs): a review. *Materials Research and Technology*, *4*(3), 333–347.

Lazzeri, A. (2016). *CVI Processing of Ceramic Matrix Composites*.

Lee, S. G., Fourcade, J., Latta, R., & Solomon, A. A. (2008). Polymer impregnation and pyrolysis process development for improving thermal conductivity of SiCp / SiC – PIP matrix fabrication. *Fusion Engineering and Design*, *83*, 713–719.

Li, X., Gao, M., & Zhang, L. (2016). Microstructure and properties of alumina ceramics prepared from submicrometer alumina powder with MgO–ZrO2 coated on alumina grain surface. *Journal of Alloys and Compounds*.

Low, I. M. (2014). *Advances in ceramic matrix composites: an introduction*. *Advances in ceramic matrix composites*. Woodhead Publishing Limited.

Masson, B. (2008). The Alumina Matrix Composite After Six Years of Use in Total Hip Arthroplasty The Alumina Matrix Composite After Six Years of Use in Total Hip Arthroplasty, 68–70.

Matikainen, V., Niemi, K., Koivuluoto, H., & Vuoristo, P. (2014). Abrasion, Erosion and Cavitation Erosion Wear Properties of Thermally Sprayed Alumina Based Coatings, 18–36.

Merchant, S. (2011). Visco-elastic properties of chitosan – titania nano-composites. *Carbohydrate Polymers*, *85*(2), 356–362.

Mujahid, M. et al. (1999). Processing and Microstructure of Alumina-Based Composites, *8*(August), 496–500.

Nassar, A. E., & Nassar, E. E. (2015). Properties of Aluminum matrix Nano composites prepared by powder metallurgy processing. *Journal of King Saud University - Engineering Sciences*.

Ogawa, F., & Masuda, C. (2015). Microstructure evolution during fabrication and microstructure-property relationships in vapour-grown carbon nanofibre-reinforced aluminium matrix composites fabricated via powder metallurgy. *Composites Part A: Applied Science and Manufacturing*, *71*, 84–94.

Oungkulsolmongkol. (2010). Hardness and Fracture Toughness of Alumina-Based Particulate Composites with Zirconia and Strontia Additives. *Journal of Metals, Materials and Minarels*, *20*(2), 71–78.

P.C Angelo, R. S. (2012). *Powder metallurgy*.

Panelli, R., & Ambrozio Filho, F. (2001). A study of a new phenomenological compacting equation. *Powder Technology*, *114*(1–3), 255–261.

Park, H. Y., Kilicaslan, M. F., & Hong, S. J. (2012). Effect of multiple pressures by magnetic pulsed compaction (MPC) on the density of gas-atomized Al-20Si powder. *Powder Technology*, *224*, 360–364.

Pi, H., Fan, S., & Wang, Y. (2012). C / SiC – ZrB 2 – ZrC composites fabricated by reactive melt infiltration with ZrSi 2 alloy. *Ceramics International*, *38*, 6541–6548.

Pournaderi, S., Mahdavi, S., & Akhlaghi, F. (2012). Fabrication of Al / Al_2O_3 composites by in-situ powder metallurgy (IPM). *Powder Technology*, *229*, 276–284.

Rocha Rangel, E. (2010). Alumina-based composites strengthened with titanium and titanium carbide dispersions. *Materials Technology*, 2010.

Rocha-rangel, E., Refugio-garcía, E., Miranda-hernández, J., & Terres-rojas, E. (2014). Alumina-based composites reinforced with silver particles. *Advances in Material*, *2*(6), 62–65.

Sakka, S., Bouaziz, J., & Ayed, F. Ben. (2014). Sintering and mechanical properties of the alumina – tricalcium phosphate – titania composites. *Materials Science & Engineering C*, *40*, 92–101.

Somani, V. (2006). *Alumina-Aluminium Titanate-Titania Nanocomposite: Synthesis , Sintering Studies , Assesment of Bioactivity*

Sun, L., Oguz, B., & Kwon, P. (2009). Powder mixing effect on the compaction capabilities of ceramic powders. *Powder Technology*, *195*(3), 227–234.

Tahara, T., Imajyo, Y., Bayu, A., Nandiyanto, D., Ogi, T., & Iwaki, T. (2014). Low-energy bead-milling dispersions of rod-type titania nanoparticles and their optical properties. *Advance Powder Metallurgy*

Tan, A. W., Pingguan-murphy, B., Ahmad, R., & Akbar, S. A. (2012). Review of titania nanotubes : Fabrication and cellular response. *Ceramics International*, *38*(6), 4421–4435.

Trent, E. M. (2015). *Metal cutting*.

Vijayaraghavan, L. (2007). Machining Of Composites An Overview. *Design and Manufacturing Technologies*, *1*(1), 16–23.

Wang, D., Dong, S., Zhou, H., Kan, Y., Wang, Z., Zhu, G., … Cao, Y. (2016). Effect of pyrolytic carbon interface on the properties of 3D C / ZrC – SiC composites fabricated by reactive melt in fi ltration. *Ceramics International*, (Cvi), 1–7.

Wang, J., Qu, X., Yin, H., Yi, M., & Yuan, X. (2008). Effect of particle size distribution on green properties during high velocity compaction. *Frontiers of Materials Science in China*, *2*(4), 392–396.

Wang, Q. (2015). Researchers predict properties of surface structure of known catalyst, (January), 2015–2016.

Wang, X., Zak Fang, Z., & Koopman, M. (2015). The relationship between the green density and as-sintered density of nano-tungsten compacts. *International Journal of Refractory Metals and Hard Materials*, *53*, 134–138.

Wildan, M., Edrees, H. J., & Hendry, A. (2002). Ceramic matrix composites of zirconia reinforced with metal particles. *MaterialsChemistry and Physics*, *75*, 276–283.

William D. Callister, D. G. R. (2011). *Material Science and Engineering 8th Edition*.

Yang, K., Rong, J., Liu, C., Zhao, H., Tao, S., & Ding, C. (2015). Study on erosion-wear behavior and mechanism of plasma-sprayed alumina-based coatings by a novel slurry injection method. *Tribiology International*.

Yang, Y., Wang, Y., Wang, Z., Liu, G., & Tian, W. (2008). Preparation and sintering behaviour of nanostructured alumina / titania composite powders modified with nano-dopants. *Materials Science and Engineering*, *490*, 457–464.

Yin, J., Lee, S., Feng, L., Zhu, Y., Liu, X., & Huang, Z. (2015). The effects of SiC precursors on the microstructures and mechanical properties of SiC f / SiC composites prepared via polymer impregnation and pyrolysis process. *Ceramics International*, *41*(3), 4145–4153.

Zhao, J. (2014). *The use of ceramic matrix composites for metal cutting applications*. *Advances in ceramic matrix composites*. Woodhead Publishing Limited.

Zou, L., Wali, N., Yang, J., & Bansal, N. P. (2010). Microstructural development of a C f / ZrC composite manufactured by reactive melt infiltration. *Journal of the European Ceramic Society*, *30*(6), 1527–1535.

APPENDIX A

CALCULATIONS

A.1 Calculation of Green Density (GD) of bulk composite

To calculate GD of the composites equation below was used, below is the example to calculate GD for 15 h of milling:

$$GD = \frac{m}{V}$$

$$= \frac{1.083g}{0.409mm^3}$$

$$= 2.648 gmm^{-3}$$

A.2 Calculation of Densification Parameter (DP) of bulk composite

To calculate DP of the composites equation below was used, below is the example to calculate GD for 15 h of milling:

$$\text{Densification} = \frac{GD - AD}{TD - AD}$$

$$= \frac{2.648 - 1.007}{3.89 - 1.007} \frac{gcm^{-3}}{gcm^{-3}}$$

$$= 0.564$$

APPENDIX B

TABLES

B.1 Green Density

Pressure	15 h	30 h	45 h	60 h
200MPa	2.648	2.637	2.665	2.664
400 MPa	2.799	2.757	2.784	2.839
600 MPa	2.85	2.864	2.864	2.928
800 MPa	2.933	2.906	2.906	2.97

B.2 Densification Parameter

Pressure	15 h	30 h	45 h	60 h
200MPa	0.551	0.564	0.577	0.552
400 MPa	0.603	0.603	0.615	0.61
600 MPa	0.62	0.637	0.656	0.64
800 MPa	0.648	0.651	0.678	0.654

APPENDIX C

FIGURE

C.1 XRD Analysis of Al_2O_3-TiO_2 composite powder mixture